



## The fumarolic CO<sub>2</sub> output from Pico do Fogo volcano (Cape Verde)

Journal:	<i>Italian Journal of Geosciences</i>
Manuscript ID	IJG-2020-0838.R1
Manuscript Type:	Original Article
Date Submitted by the Author:	n/a
Complete List of Authors:	<p>Aiuppa, Alessandro; Università di Palermo Dipartimento di Scienze della Terra e del Mare,                      Bitetto, Marcello; Università di Palermo Dipartimento di Scienze della Terra e del Mare                      Rizzo, Andrea; Istituto Nazionale di Geofisica e Vulcanologia Sezione di Palermo                      Viveiros, Maria; Instituto de Investigação em Vulcanologia e Avaliação de Riscos                      Allard, Patrick; Institut de Physique du Globe de Paris                      Frezzotti, Maria Luce; Università degli Studi di Milano-Bicocca Dipartimento di Scienze dell'Ambiente e del Territorio e di Scienze della Terra                      Valenti, Virginia; Università degli Studi di Milano-Bicocca Dipartimento di Scienze dell'Ambiente e del Territorio e di Scienze della Terra                      Zanon, Vittorio; Instituto de Investigação em Vulcanologia e Avaliação de Riscos</p>
Keywords:	Pico do Fogo volcano, Cape Verde, volcanic gases, CO <sub>2</sub> output

SCHOLARONE™  
Manuscripts

# The fumarolic CO<sub>2</sub> output from Pico do Fogo volcano (Cape Verde)

Alessandro Aiuppa<sup>1,\*</sup>, Marcello Bitetto<sup>1</sup>, Andrea L. Rizzo<sup>2</sup>, Fatima Viveiros<sup>3</sup>,

Patrick Allard<sup>4</sup>, Maria Luce Frezzotti<sup>5</sup>, Virginia Valenti<sup>5</sup>, Vittorio Zanon<sup>3,4</sup>

<sup>1</sup>*Dipartimento DiSTeM, Università di Palermo, Italy*

<sup>2</sup>*Istituto Nazionale di Geofisica e Vulcanologia, Sezione di Palermo, Italy*

<sup>3</sup>*Instituto de Investigação em Vulcanologia e Avaliação de Riscos, University of the Azores, Portugal*

<sup>4</sup>*Institute de Physique du Globe de Paris, Université de Paris, France*

<sup>5</sup>*Dipartimento di Scienze dell'Ambiente e della Terra, Università di Milano Bicocca, Italy*

\*Corresponding author: [alessandro.aiuppa@unipa.it](mailto:alessandro.aiuppa@unipa.it)

## ABSTRACT

Pico do Fogo volcano, in the Cape Verde archipelago off the western coasts of Africa, has been the most active volcano in the Macaronesia region in the Central Atlantic, with at least 27 eruptions during the last 500 years. Between eruptions fumarolic activity has been persisting in its summit crater, but limited information exists for the chemistry and output of these gas emissions. Here, we use the results acquired during a field survey in February 2019 to quantify the quiescent summit fumaroles' volatile output for the first time. Combining measurements of the fumarole compositions (using both a portable Multi-GAS and direct sampling of the hottest fumarole) and of the SO<sub>2</sub> flux (using near-vent UV Camera recording), we quantify a daily output of 1060±340 tons CO<sub>2</sub>, 780±320 tons H<sub>2</sub>O, 6.2±2.4 tons H<sub>2</sub>S, 1.4±0.4 tons SO<sub>2</sub> and 0.05±0.022 tons H<sub>2</sub>. We show that the fumarolic CO<sub>2</sub> output from Pico do Fogo exceeds (i) the time-averaged CO<sub>2</sub> release during 2015-type recurrent eruptions and (ii) is larger than current diffuse soil degassing of CO<sub>2</sub> on Fogo Island. When compared to worldwide volcanoes in quiescent hydrothermal-stage, Pico do Fogo is found to rank among the strongest CO<sub>2</sub> emitters. Its substantial CO<sub>2</sub> discharge implies a continuous deep

1  
2  
3 27 supply of magmatic gas from the volcano's plumbing system (verified by the low but measurable  
4  
5 28 SO<sub>2</sub> flux), that becomes partially affected by water condensation and sulphur scrubbing in fumarolic  
6  
7  
8 29 conduits prior to gas exit. Variable removal of magmatic H<sub>2</sub>O and S accounts for both spatial  
9  
10 30 chemical heterogeneities in the fumarolic field and its CO<sub>2</sub>-enriched mean composition, that we  
11  
12 31 infer at 64.1±9.2 mol. % H<sub>2</sub>O, 35.6±9.1 mol. % CO<sub>2</sub>, 0.26±0.14 mol. % total Sulfur (S<sub>t</sub>), and  
13  
14 32 0.04±0.02 mol. % H<sub>2</sub>.

16

17 33  
18  
19 34 **Keywords:** *Pico do Fogo volcano; Cape Verde, volcanic gases, CO<sub>2</sub> output*

20

## 21 35 22 36 23 37 24 38 INTRODUCTION

25 39  
26 40 Together with tectonic degassing, subaerial volcanism is the primary outgassing mechanism of  
27 41 mantle-derived CO<sub>2</sub> to the atmosphere (WERNER *et alii*, 2019; FISCHER *et alii*, 2019). Over  
28 42 geological time, tectonic and volcanic degassing have been the primary mechanisms for carbon  
29 43 exchange in and out our planet (DASGUPTA AND HIRSCHMANN, 2010; DASGUPTA, 2013; WONG *et*  
30 44 *alii*, 2019), ultimately playing a control role on pre-industrial atmospheric CO<sub>2</sub> levels and the  
31 45 climate (VAN DER MEER *et alii*, 2014; BRUNE *et alii*, 2017). Although attempts to estimate the global  
32 46 volcanic CO<sub>2</sub> output started early back in the 1990s (e.g., GERLACH, 1991), substantial budget  
33 47 refinements have only recently arisen from the 8-years (2011-2019) DECADE (Deep Earth Carbon  
34 48 Degassing; <https://deepcarboncycle.org/about-decade>) research program of the Deep Carbon  
35 49 Observatory (<https://deepcarbon.net/project/decade#Overview>) (FISCHER, 2013; FISCHER *et alii*,  
36 50 2019).

37 51 One key result of DECADE-funded research has been the recognition that the global CO<sub>2</sub> output  
38 52 from subaerial volcanism is predominantly sourced from a relatively small number of strongly  
39 53 degassing volcanoes. AIUPPA *et alii*, (2019) showed that the top 91 SO<sub>2</sub> volcanic emitters in 2005-  
40 54 2015 (those systematically detected from space; CARN *et alii*, 2017) produce a cumulative CO<sub>2</sub>  
41 55  
42 56  
43 57  
44 58  
45 59  
46 60

1  
2  
3  
4  
5  
6  
7  
8  
9  
10  
11  
12  
13  
14  
15  
16  
17  
18  
19  
20  
21  
22  
23  
24  
25  
26  
27  
28  
29  
30  
31  
32  
33  
34  
35  
36  
37  
38  
39  
40  
41  
42  
43  
44  
45  
46  
47  
48  
49  
50  
51  
52  
53  
54  
55  
56  
57  
58  
59  
60

release of ~39 Tg/yr, nearly half of which (~19 Tg CO<sub>2</sub>/yr) is produced by only 7 top-degassing volcanoes. It has also been found, however, that a non-trivial CO<sub>2</sub> output is additionally sustained by fumarolic degassing (FISCHER *et alii*, 2019; WERNER *et alii.*, 2019) and groundwater transport (TARAN, 2009; TARAN AND KALACHEVA, 2019) at hydrothermal volcanoes in quiescent stage. These low-temperature (hydrothermal) fumarolic emissions typically release CO<sub>2</sub> in the absence of easily detectable (by Ultra Violet (UV) spectroscopy) SO<sub>2</sub>, implying that traditional “indirect” CO<sub>2</sub> flux quantification using the volcanic gas CO<sub>2</sub>/SO<sub>2</sub> ratio proxy in tandem with remotely sensed SO<sub>2</sub> fluxes (e.g. WERNER *et alii*, 2019) cannot be employed; more challenging airborne (WERNER *et alii*, 2009) or ground-based (PEDONE *et alii*, 2014; AIUPPA *et alii*, 2015; QUEIBER *et alii*, 2016) “direct” CO<sub>2</sub> flux measurements are required instead. These technical limitations have prevented us from establishing a robust catalogue for fumarolic CO<sub>2</sub> outputs, as <50 of the several hundred degassing volcanoes in “hydrothermal-stage” worldwide have been measured for their CO<sub>2</sub> flux (WERNER *et alii*, 2019). As a consequence, the extrapolated current inventories for the global fumarolic hydrothermal CO<sub>2</sub> flux (from 15 to 35 Tg CO<sub>2</sub>/yr; FISCHER *et alii*, 2019; WERNER *et alii*, 2019) still involve very large uncertainties. In addition, most of the available information is for low-temperature arc volcanic gases, while much less is known for the fumarolic CO<sub>2</sub> output for non-arc settings (divergent, intra-plate or continental rift; e.g., ILYINSKAYA *et alii*, 2015, 2018).

Pico do Fogo, in the Cape Verde archipelago, makes part of the Macaronesia region, an area of the Atlantic Ocean off the western coasts of Africa also including the archipelagos of the Azores, Madeira and Canary (Fig. 1). This 2829 m a.s.l high strato-volcano (Fig. 2a), located on the island of Fogo, has been the most frequently erupting volcanic centre of the Macaronesia region in the last 500 years (RIBEIRO, 1960). All historical eruptions occurred on its upper flanks or in its summit crater. Between eruptions, the summit crater of Pico do Fogo hosts a persistent fumarolic field (Fig. 2b-e), with several gas vents ranging in temperature from boiling to >200°C (DIONIS *et alii*, 2014; MELIÁN *et alii*, 2015). The CO<sub>2</sub> output sustained by diffuse degassing across the crater floor was

1  
2  
3 77 estimated in the range  $147\pm 35$  (in 2009) to  $219\pm 36$  t/d (in 2010) (DIONIS *et alii*, 2014, 2015), but no  
4  
5 78 comparable data yet exists for the fumarolic CO<sub>2</sub> output itself.  
6  
7

8 79 Here we fill this gap of knowledge by presenting the very first results for the fumarolic output of  
9  
10 80 CO<sub>2</sub> and other volatiles from Pico do Fogo. These results were obtained from a gas survey on  
11  
12 81 February 5, 2019, during which we combined real-time in-situ measurement of the crater gas  
13  
14 82 compositions (Multi-GAS), direct sampling of the hottest fumarole, and near-vent remote sensing of  
15  
16 83 the SO<sub>2</sub> flux with an UV Camera. Our new data set contributes to improved quantification and  
17  
18 84 understanding of Fogo's quiescent degassing during the multi-decadal phases separating eruptions,  
19  
20 85 and offers an interesting comparison with the gas output measured during the recent 2014-2015  
21  
22 86 eruption (HERNÁNDEZ *et alii*, 2015). More broadly, our results for Pico do Fogo add a novel piece  
23  
24 87 of information to the still fragmentary data base for fumarolic CO<sub>2</sub> emissions from global volcanoes  
25  
26 88 in hydrothermal stage.  
27  
28  
29  
30  
31  
32

### 33 90 **FOGO ISLAND AND PICO DO FOGO VOLCANO**

34  
35 91 The Cape Verde archipelago, extending between 15 and 17°N latitude 500 km to the west of  
36  
37 92 Senegal, is composed of 10 main islands that are the emerged portions of a high oceanic plateau (2  
38  
39 93 km above the sea floor). Fogo Island is located at the south-western edge of this system (Fig. 1).  
40  
41 94 The Cape Verde oceanic Rise, the world's largest geoid and bathymetric seafloor anomaly  
42  
43 95 (COURTNEY & WHITE, 1986), has been interpreted as due to a hot-spot mantle swell centred north-  
44  
45 96 east of the Sal island (CROUGH, 1978, 1982; HOLM *et alii*, 2008). The presence of an active mantle  
46  
47 97 plume beneath the northern part of Cape Verde at least has been suggested by some authors based  
48  
49 98 on seismic imaging (MONTELLI *et alii*, 2006; LIU & ZHAO, 2014; SAKI *et alii*, 2015). A mantle  
50  
51 99 plume contribution is also consistent with high primordial <sup>3</sup>He (<sup>3</sup>He/<sup>4</sup>He ratios up to 12.3-15.7 Ra)  
52  
53  
54 100 in volcanics from Sao Vicente and Sao Nicolau islands (CHRISTENSEN *et alii*, 2001; DOUCELANCE *et*  
55  
56 101 *alii*, 2003; MATA *et alii*, 2010; MOURÃO *et alii*, 2012). However, a plume origin for Macaronesian  
57  
58  
59  
60

1  
2  
3 102 volcanism is still matter of debate (BONATTI, 1990; ASIMOV *et alii*, 2004), and the role of  
4  
5 103 decompressional melting (MÉTRICH *et alii*, 2014) favoured by extensional lithospheric  
6  
7  
8 104 discontinuities (MARQUES *et alii*, 2013) has received increased attention recently. Volcanism on the  
9  
10 105 Cape Verde Islands is thought to have started 24–22 Ma ago on the northeastern islands, followed  
11  
12 106 by a more recent westward migration of volcanic activity (both in the northern and southern  
13  
14  
15 107 branches of the archipelago) during the Pliocene-Pleistocene (HOLM *et alii*, 2008). Erupted products  
16  
17 108 spread a large compositional range but mafic, silica-undersaturated lavas (basanites, tephrites, and  
18  
19 109 nephelinites) prevail (GERLACH *et alii*, 1988; DAVIES *et alii*, 1989; HOLM *et alii*, 2006), eventually  
20  
21 110 associated with rarer carbonatites (KOGARKO *et alii*, 1992; HOERNLE *et alii*, 2002). Trace-element  
22  
23  
24 111 and isotope geochemistry of the erupted volcanics are extremely heterogeneous, with significant  
25  
26 112 differences between the northern and southern islands, implying the probable involvement of  
27  
28 113 several distinct mantle sources: a lower mantle plume containing both mixed HIMU (High  
29  
30  
31 114  $\mu = {}^{238}\text{U}/{}^{204}\text{Pb}$  at zero age) and EM1 (Enriched Mantle 1) end-members, possibly a 1.6-Ga  
32  
33 115 recycled oceanic crust, plus the depleted upper mantle (northern islands) and the subcontinental  
34  
35 116 lithospheric mantle (southern islands) (GERLACH *et alii*, 1988; DAVIES *et alii*, 1989; HOLM *et alii*,  
36  
37 117 2006; CHRISTENSEN *et alii*, 2001; DOUCELANCE *et alii*, 2003; MILLET *et alii*, 2008). The actual  
38  
39  
40 118 relative proportions of each of these sources are still debated however.

41  
42 119 Fogo Island (Fig. 1b), formed during the last 3–4.5 Ma, has been the single site of historical  
43  
44  
45 120 volcanic activity (27 reported eruptions) since the discovery of the Cape Verde archipelago in the  
46  
47 121 XV<sup>th</sup> century. The dominant structure of the island is Monte Amarelo volcano, whose summit was  
48  
49 122 truncated by three massive flank collapses between ca. 60 and 43 ka (Fig. 1b) (DAY *et alii*, 1999;  
50  
51 123 2000; MARQUES *et alii*, 2020). The post-collapse (62 ka to present) activity has been primarily  
52  
53  
54 124 concentrated within the Chã das Caldeiras depression (Fig. 1b), leading to progressive infilling of  
55  
56 125 the collapse scar and the formation of the Pico do Fogo cone. The cone itself (Fig. 2a) has remained  
57  
58 126 the primary eruptive centre until 1785 (RIBEIRO, 1960), when fissure-fed effusive eruptions became  
59  
60

1  
2  
3 127 concentrated along the flanks of Pico, occurring at an average frequency of one every ~50 years.  
4  
5 128 The most recent eruptions happened in 1951 (HILDNER *et alii*, 2012), 1995 (HILDNER *et alii*, 2011)  
6  
7  
8 129 and 2014-2015 (CARRACEDO *et alii*, 2015; CAPPELLO *et alii*, 2016; RICHTER *et alii*, 2016; MATA *et*  
9  
10 130 *alii*, 2017). Eruptive products of the Amarelo-Fogo volcanic complex are primarily alkali-rich  
11  
12 131 tephritic to basanitic lavas (with rarer foidites and more evolved phonolites). They are thought to  
13  
14  
15 132 ascend from a 16–28 km deep magma storage zone, emplaced in the underlying lithospheric mantle  
16  
17 133 (GERLACH *et alii*, 1988; DOUCELANCE *et alii*, 2003; HILDNER *et alii*, 2011, 2012; MATA *et alii*,  
18  
19 134 2017).

## 24 136 MATERIALS AND METHODS

25  
26 137 On February 5, 2019 we realized extensive field investigations and measurements of the summit  
27  
28 138 crater fumarolic emissions of Pico de Fogo volcano (Fig. 2a-e). We used a portable Multi-  
29  
30  
31 139 component Gas Analyser System (Multi-GAS) to analyse in real-time the fumaroles' compositions  
32  
33 140 during walking traverses across the fumarolic field (see the track shown in Figure 2e). The walking  
34  
35 141 traverse mode, first used on Vulcano Island (AIUPPA *et alii*, 2005a), is ideal to explore the chemical  
36  
37 142 heterogeneity of a fumarolic field as a high number of fumarolic vents can sequentially be analysed  
38  
39  
40 143 while slowly moving along the path. During the traverse, the Multi-GAS continuously acquired data  
41  
42 144 at 0.5 Hz, and its position was synchronously geo-localized with an embedded GPS. In addition to  
43  
44  
45 145 areas of diffuse soil degassing, 17 main fumarolic vents, showing the strongest emissions, were  
46  
47 146 identified during the traverse (Fig. 2e). Gas composition at each of these vents was determined  
48  
49 147 (Tab. 1) by keeping the MultiGAS inlet at a constant position (and for a few minutes) at about ~50  
50  
51 148 cm height above the fumarolic vent. Our Multi-GAS instrument comprised the following sensor  
52  
53  
54 149 combination (e.g., AIUPPA *et alii*, 2016): a Gascard EDI030105NG infra-red spectrometer for CO<sub>2</sub>  
55  
56 150 (Edinburgh Instruments; range: 0-30,000 ppmv); 3 electrochemical sensors for SO<sub>2</sub> (T3ST/F-  
57  
58 151 TD2G-1A), H<sub>2</sub>S (T3H-TC4E-1A) and H<sub>2</sub> (T3HYT- TE1G-1A), all from City Technology; and a  
59  
60



1  
2  
3 152 KVM3/5 Galltec-Mela temperature (T) and relative humidity (Rh) sensor. H<sub>2</sub>O concentration in the  
4  
5  
6 153 fumarolic gases was calculated from co-acquired T, Rh and pressure readings using the Arden Buck  
7  
8 154 equation (see AIUPPA *et alii*, 2016). Reading from the H<sub>2</sub>S sensor were corrected for 14% cross-  
9  
10 155 sensitivity to SO<sub>2</sub>. Gas ratios in each of the main fumaroles (Tab. 1) were derived from scatter plots  
11  
12 156 of the gas concentrations using the Ratiocalc software (TAMBURELLO, 2015). Uncertainties in all  
13  
14  
15 157 derived ratios are <15%, except for H<sub>2</sub>O/H<sub>2</sub>S ( $\leq 25\%$ ).

16  
17 158 The fumarole 15, displaying the highest emission temperature (T = 315°C), was sampled for dry  
18  
19 159 gases only by inserting a titanium tube 50 cm-long into the vent. This tube was connected to both a  
20  
21  
22 160 quartz line equipped with a condenser in order to remove water vapour and a three-way valve with a  
23  
24 161 syringe allowing to force gas flow into the line. Three dry gas samples were stored in glass bottles  
25  
26 162 equipped of two stopcocks and then moved to the INGV laboratory in Palermo for chemical  
27  
28  
29 163 analysis. Concentrations of He, H<sub>2</sub>, O<sub>2</sub>, N<sub>2</sub>, CO, CH<sub>4</sub>, CO<sub>2</sub> and H<sub>2</sub>S were determined using a gas  
30  
31 164 chromatograph (Clarus 500, Perkin Elmer) equipped with a 3.5-m column (Carboxen 1000) and a  
32  
33 165 double detector (hot-wire detector and flame ionization detector [FID]). SO<sub>2</sub> was not measurable  
34  
35 166 with this sampling/analytical setup. Analytical errors were <3%. The results are reported in Tab. 2.

36  
37 167 Simultaneously to our Multi-GAS traverse, we also operated a portable dual UV camera system  
38  
39  
40 168 for measuring the volcanic SO<sub>2</sub> flux. The camera system registered at 0.5 Hz for ~100 minutes from  
41  
42 169 a fixed position on the inner crater terrace's rim, deep inside the summit crater (see Figs. 2b, 2e).  
43  
44  
45 170 The system used two co-aligned cameras (JAI CM-140GE-UV), both fitted with optical lenses of  
46  
47 171 45° Field of View, and mounting two different band-pass optical filters with Full Width at Half  
48  
49 172 Maximum (FWHM) of 10 nm and central wavelengths of 310 and 330 nm, respectively. The filters  
50  
51  
52 173 were applied in front of the cameras so to achieve differential UV absorption in the SO<sub>2</sub> band  
53  
54 174 (KANTZAS *et alii*, 2009; KERN *et alii*, 2010; DELLE DONNE *et alii*, 2019). The system, housed in a  
55  
56 175 peli case and powered by a 12V LiPo battery, was mounted on a tripod and rotated to look upward  
57  
58 176 to image the crater's inner northern slope (where the fumarolic field is located) and a portion of the  
59  
60



1  
2  
3 177 background sky (Figs. 2b, 2d). Data acquisition was commanded via PC using the Vulcamera  
4  
5 178 software (TAMBURELLO *et alii* 2011). The acquired images (520x676 pixels at 10-bit resolution)  
6  
7  
8 179 were post-processed using standard techniques (KANTZAS *et alii*, 2009; TAMBURELLO *et alii*, 2011,  
9  
10 180 2012): sets of co-acquired images were combined into absorbance images and were then converted  
11  
12 181 into SO<sub>2</sub> slant column amount (SCA) images by successively using three different calibration cells.  
13  
14  
15 182 Finally, we derived an Integrated Column Amount (ICA) time-series by integrating the SCA along  
16  
17 183 the cross-section shown in Fig. 2b and then the SO<sub>2</sub> flux by multiplying the ICA with the plume  
18  
19 184 speed. The plume speed ( $1.9 \pm 0.6$  m/s) was obtained by processing image sequences acquired at 0.2  
20  
21  
22 185 Hz using a LifeCam Cinema HD (Microsoft) USB visible camera, integrated in the UV Camera  
23  
24 186 system. Processing involved quantifying the rising speeds of ~50 individual gas puffs of well-  
25  
26 187 resolved structure, moving upward from the fumarolic field toward the crater edge (Fig. 2d).

28  
29 188 Finally, from the same position as the UV camera, we used a portable handheld thermal camera  
30  
31 189 (model FLIR E5) in order to acquire a thermal map of the fumarolic field (see Fig. 2b). This map  
32  
33 190 allowed us to verify that the hottest degassing areas were in large part covered by the Multi-GAS  
34  
35 191 traverse. Temperatures of fumaroles 5 and 14-15, the hottest vents in the field (Fig. 2b), were also  
36  
37  
38 192 directly measured in situ with a portable thermocouple.

## 42 194 RESULTS

### 44 195 FUMAROLIC GAS COMPOSITION: MULTI-GAS AND DIRECT SAMPLING

46  
47 196 As a whole, during the ~74-minute duration of our Multi-GAS traverse we obtained 4446  
48  
49 197 simultaneous measurements of H<sub>2</sub>O, CO<sub>2</sub>, SO<sub>2</sub>, H<sub>2</sub>S and H<sub>2</sub> concentrations in Fogo gas emissions  
50  
51 198 (one analysis every 2 seconds). The entire dataset is illustrated in Figure 3 where the gas  
52  
53  
54 199 concentrations in the near-vent fumarolic plumes are displayed as scatter plots. The concentrations  
55  
56 200 of H<sub>2</sub>O, CO<sub>2</sub> and H<sub>2</sub> were corrected for the respective air background values of ~12,000, ~600 and  
57  
58 201 ~0.5 ppmv measured upwind (outside) the fumarolic field (Fig. 2e). The high background CO<sub>2</sub>  
59  
60

1  
2  
3 202 concentration compared to “normal” atmosphere (~400 ppmv) is explained by the high diffuse soil  
4  
5 203 CO<sub>2</sub> emission through the inner crater floor (DIONIS *et alii*, 2014, 2015).

7  
8 204 The absolute gas concentrations measured along our traverse display quite large variations (Fig.  
9  
10 205 3), indicating chemical heterogeneity in the fumarolic field emissions. This is especially evident in  
11  
12 206 the SO<sub>2</sub> vs. H<sub>2</sub>S scatter plot (Fig. 3). Otherwise, one observes broad co-variations among most gas  
13  
14 207 species, even though with some spread. The maximum peak values reached ~23,000 (H<sub>2</sub>O),  
15  
16  
17 208 ~20,000 (CO<sub>2</sub>), 118 (H<sub>2</sub>S), 62 (SO<sub>2</sub>) and 30 (H<sub>2</sub>) ppmv.

19 209 The molar compositions of fumarolic gases from the 17 individualized vents (Tab. 1) confirm  
20  
21 210 this spatial heterogeneity. Each fumarole actually exhibited stable, well-resolved composition (see  
22  
23  
24 211 the fumarole 15 example in Figure 3). Instead, the SO<sub>2</sub>/H<sub>2</sub>S ratios in all fumaroles span more than  
25  
26 212 three orders of magnitude, from 0.001 to 1.5 (Tab. 1 and Fig. 3). The H<sub>2</sub>O/H<sub>2</sub>S, CO<sub>2</sub>/H<sub>2</sub>S, and  
27  
28 213 H<sub>2</sub>/H<sub>2</sub>S also varied considerably within the fumarolic field, with respective ranges of 98-480, 108-  
29  
30  
31 214 240 and 0.05-0.24 (Tab. 1 and Fig. 3).

33 215 Table 2 shows the chemistry of dry gases collected from the hottest (315°C) F15 fumarole (Fig.  
34  
35 216 2d, e). CO<sub>2</sub> is the overwhelming component (up to 97%), followed by H<sub>2</sub>S (around 1%), H<sub>2</sub> (952-  
36  
37 217 979 ppm), CO (15-17 ppm) and CH<sub>4</sub> (around 1-2 ppm). N<sub>2</sub> and O<sub>2</sub> contents reflect air  
38  
39 218 contamination of the samples, with minimum values of 0.5% and 0.1%. The concentration of  
40  
41  
42 219 helium is around 8 ppm in our less contaminated sample. Whatever the degree of air contamination,  
43  
44 220 our samples from the hottest F15 fumarole reveal CO<sub>2</sub>/H<sub>2</sub>S (94-107) and H<sub>2</sub>/H<sub>2</sub>S (0.09-0.10) ratios  
45  
46  
47 221 (Tab. 2) that are very comparable to the corresponding ratios determined with Multi-GAS.

49 222 The SO<sub>2</sub>/H<sub>2</sub>S ratio is a commonly used marker to distinguish the magmatic (SO<sub>2</sub>-rich) vs.  
50  
51 223 hydrothermal (H<sub>2</sub>S-rich) nature of volcanic gas (e.g. AIUPPA *et alii*, 2005b). Figure 4 shows that  
52  
53  
54 224 Pico do Fogo fumaroles define a nearly continuous trend from two end-members:

56 225 (i) a magmatic end-member, represented by the hottest gas from fumaroles 14-15 (T = 315-316  
57  
58 226 °C), characterized by H<sub>2</sub>O/CO<sub>2</sub> of ~ 2, CO<sub>2</sub>/S<sub>t</sub> of ~ 100, high SO<sub>2</sub> (~0.2 mol. %) and

60

1  
2  
3 227 relatively low H<sub>2</sub>S, and oxidised (redox conditions of about 1 log unit above the Nickel-  
4  
5 228 Nickel Oxide buffer at ~500°C, estimated from the measured SO<sub>2</sub>/H<sub>2</sub>S ~ 0.9-1.4 and  
6  
7  
8 229 H<sub>2</sub>/H<sub>2</sub>O ~ 0.0004; see methodology in AIUPPA et al., 2011); and,  
9

10 230 (ii) a hydrothermal end-member, represented by fumaroles 3-8, that is H<sub>2</sub>S-dominated (~0.35-  
11  
12 231 0.43 mol. %; SO<sub>2</sub>/H<sub>2</sub>S of ~ 0.01-0.2), relatively richer in CO<sub>2</sub> (CO<sub>2</sub>/S<sub>t</sub> > 130 and  
13  
14  
15 232 H<sub>2</sub>O/CO<sub>2</sub> < 1) and more reduced (H<sub>2</sub>/H<sub>2</sub>O > 0.0015) (corresponding to redox conditions  
16  
17 233 close to the FeO-FeO1.5 buffer; GIGGENBACH, 1987).  
18

19 234 The red star in Figures 4a-d represents the spatially integrated composition of Pico do Fogo's  
20  
21 235 fumarolic emission, calculated as the arithmetic mean of compositions of the 17 main fumaroles. It  
22  
23  
24 236 is characterized by the following ratios, normalized to H<sub>2</sub>S: SO<sub>2</sub>/H<sub>2</sub>S = 0.3±0.4, H<sub>2</sub>O/H<sub>2</sub>S =  
25  
26 237 299±109, CO<sub>2</sub>/H<sub>2</sub>S = 153±33 and H<sub>2</sub>/H<sub>2</sub>S = 0.2±0.04 (Tab. 1). The mean SO<sub>2</sub>/H<sub>2</sub>S ratio of ~0.3 is  
27  
28  
29 238 not much different from the SO<sub>2</sub>/H<sub>2</sub>S ratio of 0.12 of the bulk volcanic plume (Tab. 1 and Fig. 4)  
30  
31 239 determined after 30-min continuous Multi-GAS measurements made on the outer crater rim (see  
32  
33 240 "bulk plume Multi-GAS site" in Fig. 2b, e). At that Multi-GAS site, we could intercept only a very  
34  
35 241 dilute plume, rising buoyantly from the fumarolic field inside the crater floor (Fig. 2d). Only small  
36  
37  
38 242 concentrations of H<sub>2</sub>S (~ 1 ppmv) and SO<sub>2</sub> (~ 0.15 ppmv) could be detected, no volcanic H<sub>2</sub>O, CO<sub>2</sub>,  
39  
40 243 or H<sub>2</sub> being resolvable from the air background. Given these very low H<sub>2</sub>S and SO<sub>2</sub> concentrations,  
41  
42 244 well below our calibration range (10-200 ppmv), the inferred bulk plume SO<sub>2</sub>/H<sub>2</sub>S ratio of 0.12  
43  
44  
45 245 must be considered with caution; we just take it as indication that hydrothermal H<sub>2</sub>S-rich fumaroles  
46  
47 246 prevail over the more magmatic end-member fumaroles in the bulk gas emission from Pico do  
48  
49 247 Fogo, in agreement with indications from the arithmetic mean of fumarolic compositions.  
50

## 51 248 52 53 54 249 SO<sub>2</sub> FLUX

55  
56 250 Figure 5a presents the SO<sub>2</sub> flux time-series obtained by the UV Camera on February 5, 2019. A  
57  
58 251 plot of SO<sub>2</sub> column amounts along the UV cross-section of Fig. 5b shows that, thanks to the short  
59  
60

1  
2  
3 252 distance (~200 m) between the camera and the targeted plume, a feeble but continuous SO<sub>2</sub>  
4  
5 253 emission (<400 ppm·m; mean, 140±110 ppm·m) was detected by the UV Camera in the leftmost  
6  
7  
8 254 portion of the camera FoV (Fig. 5c), and persisted throughout the ~100 minutes of recording (Fig.  
9  
10 255 5a). During our measurement interval the SO<sub>2</sub> flux varied between 0.3 and 2.3 tons/day (or 0.009 to  
11  
12 256 0.06 kg/s) and averaged at 1.4±0.4 tons/day (0.016±0.004 kg/s).

## 23 24 261 **DISCUSSION**

### 25 26 262 THE COMPOSITION OF PICO DO FOGO FUMARoles

27  
28 263 The molar gas ratios determined by Multi-GAS measurements allow us to compute the molar  
29  
30  
31 264 percentages of H<sub>2</sub>O, CO<sub>2</sub>, H<sub>2</sub>S, SO<sub>2</sub> and H<sub>2</sub> in each fumarole and in the mean gas composition  
32  
33 265 (Table 1). These percentages for only the 5 above species are upper bounds since we did not  
34  
35 266 determine other possible minor species (N<sub>2</sub>, HCl) in the gases. Otherwise, they are not affected by  
36  
37  
38 267 the presence of reduced carbon species, whose amount was verified to be very low in F5 fumarole  
39  
40 268 this study and (MELIÁN *et alii*, 2015). According to our results, the Pico do Fogo fumaroles are  
41  
42 269 moderately hydrous (41-73 % H<sub>2</sub>O; mean, 64 %), CO<sub>2</sub>-rich (27-59 %; mean, 36 %), and contain  
43  
44  
45 270 about ~0.3 % S<sub>t</sub> and 0.04 % H<sub>2</sub> (Tab. 1). These mean values match well the composition of the F15  
46  
47 271 fumarole, directly sampled and analysed in laboratory, as regards the H<sub>2</sub>/H<sub>2</sub>S and CO<sub>2</sub>/H<sub>2</sub>S molar  
48  
49 272 ratios (Tab. 2).

50  
51 273 The triangular plot in Figure 6 puts the H<sub>2</sub>O-CO<sub>2</sub>-S<sub>t</sub> compositions of our Pico do Fogo fumaroles  
52  
53  
54 274 in a wider context, by comparing them against the compositions of (i) the 2014 Fogo eruption  
55  
56 275 plume (HERNÁNDEZ *et alii*, 2015), which represents the only available datum for the Fogo  
57  
58 276 magmatic gas signature to date; (ii) magmatic gases from other intraplate, rift and/or divergent-plate  
59  
60

1  
2  
3 277 volcanoes (see AIUPPA, 2015 for data sources); and (iii) fumaroles from other volcanic systems in  
4  
5 278 the Macaronesia region, including the Azores (CALIRO *et alii*, 2005; FERREIRA & OSKARSSON,  
6  
7 279 1999; FERREIRA *et alii*, 2005; MARES project, this study) and Teide in the Canary (MELIÁN *et alii*,  
8  
9 280 2012; MARES project, this study).

11  
12 281 The Pico do Fogo summit fumaroles (this study) are compositionally distinct from the magmatic  
13  
14 282 gases released during the 2014 eruption (HERNÁNDEZ *et alii*, 2015), this latter falling well within  
15  
16 283 the range of measured magmatic gas compositions at other intraplate volcanoes (yellow field, from  
17  
18 284 AIUPPA, 2015). More specifically, the summit Fogo fumaroles are evidently S-depleted relative to  
19  
20 285 the 2014 magmatic gas, which strongly suggests intense sub-surface scrubbing of reactive S  
21  
22 286 compounds under the “hydrothermal” conditions of the fumarolic field, where surface temperatures  
23  
24 287 ( $\leq 315$  °C) are well below the boiling temperature of liquid sulfur (455 °C; above which S  
25  
26 288 scrubbing become minimal, if any; AIUPPA *et alii*, 2017). Extensive S deposition in the sub-surface  
27  
28 289 environment of the summit fumaroles is further supported by  $\text{CO}_2/\text{S}_t$  ratios being far higher in the  
29  
30 290 fumaroles (93-162) than in the 2014 eruption gas (1.5; HERNÁNDEZ *et alii*, 2015) (Figs. 6, 7). The  
31  
32 291 two hottest summit fumaroles (F14 and F15) consistently display the lowest  $\text{CO}_2/\text{S}_t$  ratios (93-97),  
33  
34 292 but these are still two orders of magnitude higher than in the eruptive gas, confirming the  
35  
36 293 importance of sulfur scrubbing (Fig. 7). This is also verified for the dry gases directly sampled from  
37  
38 294 fumarole F15, whose  $\text{CO}_2/\text{H}_2\text{S}$  ratio is 94-107 (Tab. 2).

39  
40 295 Fogo summit fumaroles are also less hydrous (or more  $\text{CO}_2$ -rich) than the 2014 eruptive gas  
41  
42 296 (Fig. 6). If the 2014 gas is representative of the magmatic gas feeding the summit fumaroles (a  
43  
44 297 magmatic gas supply is indeed supported by the low but measurable  $\text{SO}_2$  output; Fig. 5), then the  
45  
46 298 simplest explanation of  $\text{H}_2\text{O}$  depletion in the fumaroles is extensive steam condensation in the  
47  
48 299 fumarolic conduits due to low temperature conditions. Because our Multi-GAS measurements were  
49  
50 300 made in air-diluted (and cooled) fumarolic plumes, we cannot entirely exclude that partial  $\text{H}_2\text{O}$   
51  
52 301 condensation could have also occurred during plume transport and/or in the Multi-GAS inlet system  
53  
54  
55  
56  
57  
58  
59  
60

1  
2  
3 302 (tubing + filter), such as previously observed at other volcano-hydrothermal systems (e.g., ALLARD  
4  
5 303 *et alii*, 2014; LOPEZ *et alii*, 2017; TAMBURELLO *et alii*, 2019). However, we note that our Multi-  
6  
7  
8 304 GAS-derived H<sub>2</sub>O range (41-73 %) partially overlaps with the H<sub>2</sub>O range (52-92 %) for the summit  
9  
10 305 Fogo fumaroles previously determined from direct gas sampling (MELIÁN *et alii*, 2015). We thus  
11  
12 306 conclude that both subsurface and within-plume H<sub>2</sub>O condensation may combine to drive the  
13  
14 307 summit fumaroles toward a less hydrous and correspondingly CO<sub>2</sub>-enriched composition compared  
15  
16  
17 308 to the 2014 eruptive gas. We cannot exclude, however, that the magmatic gas that feeds the  
18  
19 309 persistent summit fumaroles is compositionally different from the 2014 eruptive gas. If for example  
20  
21 310 the magmatic gas source is the Pico do Fogo magma reservoir located in the uppermost mantle at  
22  
23 311 16–28 km depth (HILDNER *et alii*, 2011, 2012; MATA *et alii*, 2017), then it is well possible that  
24  
25 312 its composition has deeper (CO<sub>2</sub>-richer, H<sub>2</sub>O-S-poorer) signature than that of eruptive 2014 gas  
26  
27 313 (derived from shallow degassing).  
28  
29  
30

31 314 The Pico do Fogo fumaroles plot at the CO<sub>2</sub>-rich end of the compositional array defined by  
32  
33 315 volcanic hydrothermal fluids in the Macaronesian region (Fig. 6). The majority of volcanic  
34  
35 316 fumaroles from the Azores (Sao Miguel, Terceira and Graciosa islands) and from Teide volcano in  
36  
37 317 the Canaries are shifted toward the H<sub>2</sub>O corner. This is a typical (but not exclusive) feature of most  
38  
39 318 hydrothermal steam vents worldwide (CHIODINI & MARINI, 1998), which reflects their derivation  
40  
41 319 from the boiling of meteoric groundwater-fed hydrothermal systems (CALIRO *et alii*, 2015). The  
42  
43 320 less hydrous compositions of Pico do Fogo fumaroles suggest the absence of a shallow boiling  
44  
45 321 hydrothermal aquifer underneath Pico's summit, and consequently a weaker (relative to Azores and  
46  
47 322 Teide) hydrothermal fingerprint (greater magmatic signature), especially in the hottest fumaroles  
48  
49 323 (F14 and F15) that also exhibit lower CO<sub>2</sub>/S<sub>t</sub> ratios (Fig. 7) and higher SO<sub>2</sub>/H<sub>2</sub>S ratios (Fig. 4).  
50  
51 324 These SO<sub>2</sub>-bearing F14-F15 fluids appear as formerly magmatic gases that have undergone partial  
52  
53 325 H<sub>2</sub>O-S<sub>t</sub> loss (via condensation + scrubbing) during cooling and hydrothermal re-equilibration (Fig.  
54  
55 326 6). Instead, the most SO<sub>2</sub>-poor, H<sub>2</sub>S-dominated fumaroles (e.g., F3-F8) have suffered more  
56  
57  
58  
59  
60

1  
2  
3 327 significant hydrothermal processing, as testified by their lower  $H_2O/CO_2$  ( $< 1$ ), higher  $CO_2/S_t$  ( $>$   
4  
5 328 130), and more reduced ( $H_2$ -rich) redox conditions, typical of hydrothermal fluids (FISCHER &  
6  
7  
8 329 CHIODINI, 2015) (Figs. 4, 7).

9  
10 330 To conclude, we attribute the  $CO_2$ -rich compositions of the Pico do Fogo fumaroles to a  
11  
12 331 combination of (i) hydrothermal interactions (partially removing magmatic sulphur and water) and  
13  
14  
15 332 possibly (ii) a deep magmatic gas source.

#### 16 17 333 18 19 334 GAS OUTPUT BUDGET

20  
21 335 Combining the compositional data described above with the UV camera-based  $SO_2$  flux record  
22  
23  
24 336 depicted in Figure 5, we can reliably estimate the output of  $CO_2$  and other volatiles from the summit  
25  
26 337 crater fumarolic field of Pico do Fogo (Table 3). To do this calculation, we combine the measured  
27  
28  
29 338 mean  $SO_2$  flux ( $1.4 \pm 0.4$  tons/day) and the mean molar composition of the summit fumaroles  
30  
31 339 ( $64.1 \pm 9.2$  %  $H_2O$ ,  $35.6 \pm 9.1$  %  $CO_2$ ,  $0.2 \pm 0.08$  %  $H_2S$ ,  $0.06 \pm 0.06$  %  $SO_2$ , and  $0.04 \pm 0.02$  %  $H_2$ ; red  
32  
33 340 star in Figs. 4, 6 and 7), the  $S_t$  ( $0.26 \pm 0.14$  %) of which is scaled to the bulk plume  $SO_2/H_2S$  ratio of  
34  
35 341 0.12 (Tab. 1 and Fig. 4) to infer the bulk plume mass ratios at 558 ( $H_2O/SO_2$ ), 756 ( $CO_2/SO_2$ ), 4.2  
36  
37  
38 342 ( $H_2S/SO_2$ ) and 1.1 ( $H_2/SO_2$ ), respectively. This procedure allows us to smooth the effect of the large  
39  
40 343 compositional heterogeneity of the fumarolic vents. We just note that the bulk plume  $SO_2/H_2S$  ratio  
41  
42 344 of 0.12 characterizes the predominance of  $H_2S$ -dominated (F3-F8-like) hydrothermal fluids over  
43  
44  
45 345 more  $SO_2$ -rich (F14-F15-like) “more magmatic” fumaroles.

46  
47 346 We obtain a daily fumarolic  $CO_2$  output of  $1060 \pm 340$  tons (Table 3). We also estimate a daily  
48  
49 347 release of  $780 \pm 320$   $H_2O$ ,  $6.2 \pm 2.4$   $H_2S$  and  $0.05 \pm 0.022$   $H_2$ . These results demonstrate that the  
50  
51  
52 348 fumarolic gas output is larger, for all volatiles, than diffuse degassing through the crater floor  
53  
54 349 (DIONIS *et alii*, 2014, 2015) (Fig. 8). For example, the latter has been estimated to produce 147-219  
55  
56 350 ( $\pm 35$ ) tons/day of  $CO_2$  (DIONIS *et alii*, 2014, 2015), which is only 14-20% of the inferred fumarolic  
57  
58 351  $CO_2$  output. Even considering the soil  $CO_2$  output estimated at the scale of the entire island ( $828 \pm 5$   
59  
60



1  
2  
3 352 tons/day; DIONIS *et alii*, 2015), the contribution of diffuse degassing remains less than a half (~  
4  
5 353 43%) of the total Fogo island CO<sub>2</sub> degassing budget (~1890 tons/day; this study and DIONIS *et alii*,  
6  
7  
8 354 2015).

9  
10 355 In contrast, the daily fumarolic gas output is far lower than the eruptive gas output (Fig. 8) for  
11  
12 356 the 2014 eruption derived by HERNÁNDEZ *et alii*, (2015) by combining SO<sub>2</sub> flux measurements with  
13  
14  
15 357 a scanning UV spectrometer (using the Differential Optical Absorption Spectroscopy – DOAS -  
16  
17 358 technique) and a Multi-GAS-derived plume composition. Our fumarolic SO<sub>2</sub> output, for example, is  
18  
19 359 a factor ~7000 lower than the large (~10 ktons) daily eruptive release (HERNÁNDEZ *et alii*, 2015).  
20  
21 360 Let emphasize, however, that while summit fumarolic emissions at Fogo have persisted as a stable  
22  
23  
24 361 degassing feature over the past few centuries (RIBEIRO, 1960), eruptive degassing has been  
25  
26 362 restricted to the relatively infrequent eruptions. There are only 10 reported eruptions since 1785  
27  
28  
29 363 (RIBEIRO, 1960), of which only 3 since 1951 (HILDNER *et alii*, 2011, 2012; CARRACEDO *et alii*,  
30  
31 364 2015; MATA *et alii*, 2017). Between June 12, 1951 (the onset of the first, well recorded XX century  
32  
33 365 eruption; HILDNER *et alii*, 2012) and February 8, 2015 (the end of the last eruption), Fogo has been  
34  
35 366 in eruption for only 200 days (e.g., 0.008 % of the 24710 elapsed days). If we take the November  
36  
37  
38 367 30, 2015 gas output (HERNÁNDEZ *et alii*, 2015) as typical for Fogo eruptive daily degassing rate, we  
39  
40 368 can roughly compute a cumulative eruptive release for 1951-2015 (200 days of eruption) of ~4  
41  
42 369 Mtons of H<sub>2</sub>O, ~2 Mtons of CO<sub>2</sub> and SO<sub>2</sub>, 11 ktons of H<sub>2</sub>S and 0.04 ktons of H<sub>2</sub>. These masses,  
43  
44  
45 370 when scaled to (integrated over) the 24710 days elapsed from June 12, 1951 to February 8, 2015,  
46  
47 371 correspond to daily eruptive outputs of only 196, 86, 82, 0.5 and 0.002 tons/day for H<sub>2</sub>O, CO<sub>2</sub>, SO<sub>2</sub>,  
48  
49 372 H<sub>2</sub>S and H<sub>2</sub>, respectively (Fig. 8). Our back-of-the-envelope calculations demonstrate that, when  
50  
51  
52 373 examined on longer-term perspective, eruptive emissions at Fogo are significant for only SO<sub>2</sub>, while  
53  
54 374 they do make a relatively small contribution to the emission budget of other volatiles (Fig. 8).

55  
56 375 We therefore conclude that summit crater fumarolic emissions at Pico do Fogo are the dominant  
57  
58 376 source of volcanic CO<sub>2</sub> (and most other volatiles) over multi-decadal scale.

60

377  
378 IMPLICATIONS FOR THE GLOBAL CO<sub>2</sub> OUTPUT INVENTORY

379 On a broader perspective, our results for Pico do Fogo in Cape Verde archipelago add a new  
380 piece of information to the global catalogue of volcanic CO<sub>2</sub> emissions. Recent work (FISCHER *et*  
381 *alii*, 2019; WERNER *et alii*, 2019) has attempted at refining the global volcanic CO<sub>2</sub> emission  
382 inventory, by reviewing, cataloguing and synthesizing the volcanic CO<sub>2</sub> output information  
383 available in the international literature. It was found that, by late 2019, CO<sub>2</sub> flux measurements have  
384 become available for 102 of the ~500 degassing subaerial volcanoes worldwide (FISCHER *et alii*,  
385 2019; WERNER *et alii*, 2019; FISCHER & AIUPPA, 2020 submitted). Different strategies have been  
386 used to extrapolate the cumulative CO<sub>2</sub> output “measured” for the 102 volcanoes (~44 Tg/yr) to  
387 CO<sub>2</sub> emissions from the several hundred “unmeasured” subaerial degassing volcanoes. These have  
388 included the use of independent rock-chemistry information (AIUPPA *et alii*, 2019) and/or the  
389 identification of statistical properties (mean CO<sub>2</sub> output and confidence intervals) for different  
390 categories of volcanoes. On the latter basis, it was proposed that the present-day global volcanic  
391 CO<sub>2</sub> budget is dominated by the category of Strong Volcanic Gas Emitters (S<sub>vge</sub>) – which includes  
392 the ~100 top degassing volcanoes whose SO<sub>2</sub> emissions are systematically detected from space-  
393 borne and/or ground-based spectrometers (CARN *et alii*, 2017; FISCHER *et alii*, 2019). S<sub>vge</sub> have an  
394 inferred total (extrapolated) CO<sub>2</sub> output of ~ 36-39 Tg/yr (AIUPPA *et alii*, 2019; FISCHER *et alii*,  
395 2019). It was additionally found that a group of Weak Volcanic Gas Emitters (W<sub>vge</sub>), although  
396 degassing in a more subtle manner (this category includes volcanoes with no visible plumes and/or  
397 minor to absent SO<sub>2</sub> emissions), may still contribute between 15 (FISCHER *et alii*, 2019) and 35  
398 (WERNER *et alii*, 2019) Tg CO<sub>2</sub>/yr, simply because they are numerous (~400) globally.  
399 Unfortunately, however, these results are subject to very large uncertainties because measuring the  
400 CO<sub>2</sub> output from quiescent/hydrothermal volcanoes is especially challenging from a technical

1  
2  
3 401 viewpoint (indirect SO<sub>2</sub> flux-based estimates are hampered by low to absent SO<sub>2</sub>; WERNER *et alii*,  
4  
5 402 2019), making the CO<sub>2</sub> flux catalogue particularly incomplete for W<sub>vge</sub>.

7  
8 403 Pico do Fogo falls within the W<sub>vge</sub> category, as no plume is visually observable (Fig. 2) and no  
9  
10 404 SO<sub>2</sub> is detectable by satellite except during the infrequent eruptions (GLOBAL VOLCANISM  
11  
12 405 PROGRAM, 2017). Our results show, however, that SO<sub>2</sub> is present in tiny but measurable quantities  
13  
14 406 in the fumaroles (Table 1), making both the SO<sub>2</sub> flux and, indirectly, the CO<sub>2</sub> flux (Table 3)  
15  
16  
17 407 measurable from a very proximal location on ground (Fig. 2; note that a test made with UV-Camera  
18  
19 408 from the base of the volcano were unable to detect any SO<sub>2</sub> release).

21  
22 409 When put in the context of global volcanic CO<sub>2</sub> fluxes (Fig. 9; data from FISCHER *et alii*, 2019),  
23  
24 410 the fumarolic CO<sub>2</sub> flux from Pico do Fogo (ca. 1000 tons/day) confirms that W<sub>vge</sub> volcanoes can  
25  
26 411 emit CO<sub>2</sub> in quantities that, in some cases, can rival the emissions of S<sub>vge</sub> volcanoes. High CO<sub>2</sub>  
27  
28 412 emission from such W<sub>vge</sub> systems, despite negligible (hydrothermal-dominant) to weak (magmatic-  
29  
30  
31 413 hydrothermal) SO<sub>2</sub> emission (FISCHER *et alii*, 2019), result from their exceptionally high CO<sub>2</sub>/S<sub>t</sub>  
32  
33 414 signature (AIUPPA *et alii*, 2017). Pico do Fogo fumaroles are not an exception, but owing to their  
34  
35 415 high CO<sub>2</sub>/S<sub>t</sub> compositions they can sustain a CO<sub>2</sub> output of order 1000 tons/day, at the upper range  
36  
37  
38 416 of the global W<sub>vge</sub> and S<sub>vge</sub> populations (Fig. 9). Therefore, our present results further demonstrate  
39  
40 417 that refining the global inventory for volcanic CO<sub>2</sub> output will require enhanced quantification of  
41  
42 418 the weaker, poorly visible emissions sustained by quiescent hydrothermal volcanoes, the majority of  
43  
44  
45 419 which still lack CO<sub>2</sub> flux quantification.

## 46 47 420 CONCLUSIONS

49 421 We have shown here that fumarolic activity on-top of Pico do Fogo volcano, in the Atlantic Cape  
50  
51 422 Verde archipelago, is currently a poorly visible but substantial source of volcanic volatiles to the  
52  
53  
54 423 atmosphere. The fumarolic CO<sub>2</sub> output (~1060 tons/day), in particular, is found to exceed by far the  
55  
56 424 time-integrated eruptive CO<sub>2</sub> flux (~86 tons/day) from the volcano, as well as the estimated total  
57  
58 425 CO<sub>2</sub> budget from soil degassing across Fogo island (147-828 tons/day). On a broader scale, our  
59  
60

1  
2  
3 426 results confirm that quiescent volcanoes characterized by hydrothermal activity during quiescent  
4  
5 427 stages can produce CO<sub>2</sub> emissions that rival those of more manifestly degassing (Strong Volcanic  
6  
7  
8 428 Gas Emitters, S<sub>vge</sub>) owing to their CO<sub>2</sub>-enriched fumarole compositions (CO<sub>2</sub>/S<sub>t</sub> ratios of 93-163 at  
9  
10 429 Pico do Fogo in 2019). At Pico do Fogo, these CO<sub>2</sub>-enriched compositions likely result from the  
11  
12 430 interactions (scrubbing of magmatic sulphur, and water condensation) of a deep magmatic gas  
13  
14  
15 431 supply (perhaps sourced from a 16–28 km deep magma reservoir in the uppermost mantle; HILDNER  
16  
17 432 *et alii*, 2011, 2012; MATA *et alii*, 2017) with a shallow hydrothermal system.

#### 18 19 433 20 21 434 ACKNOWLEDGEMENTS

22  
23  
24 435 This research was funded by the Portuguese Fundação para a Ciência e a Tecnologia (MARES  
25  
26 436 project - PTDC/GEO-FIQ/1088/2014), the DECADE project of the Deep Carbon Observatory, and  
27  
28 437 the Italian Ministero Istruzione Università e Ricerca (Grant n. 2017LMNLAW). We thank  
29  
30  
31 438 Francesco Salerno and Manfredi Longo from INGV-Palermo for providing support with gas  
32  
33 439 chromatographic analysis. The manuscript benefited from constructive reviews from Taryn Lopez,  
34  
35 440 Yuri Taran and from the Associate Editor Orlando Vaselli.

#### 36 37 441 38 39 40 442 REFERENCES

- 41  
42 443 AIUPPA A. (2015) - *Volcanic-gas monitoring* In: *Volcanism and Global Environmental Change*, pp.  
43  
44 444 81-96. Cambridge University Press. doi: 10.1007/9781107415683.007.
- 45  
46  
47 445 AIUPPA A., FEDERICO C., GIUDICE G. & GURRIERI S. (2005a) - *Chemical mapping of a fumarolic*  
48  
49 446 *field: La Fossa Crater, Vulcano Island (Aeolian Islands, Italy)*. Geophysical Research Letters,  
50  
51 447 **32**, 4.
- 52  
53  
54 448 AIUPPA A., INGUAGGIATO S., MCGONIGLE A.J.S., O'DWYER M., OPPENHEIMER C., PADGETT M.J.,  
55  
56 449 ROUWET D. & VALENZA M. (2005b) - *H<sub>2</sub>S fluxes from Mt. Etna, Stromboli, and Vulcano (Italy)*

- 1  
2  
3 450 *and implications for the sulfur budget at volcanoes. Geochim. Cosmochim. Acta, 69 (7), 1861-*  
4  
5  
6 451 1871.
- 7  
8 452 AIUPPA A., SHINOHARA H., TAMBURELLO G., GIUDICE G., LIUZZO M., MORETTI R., (2011) –  
9  
10 453 *Hydrogen in the gas plume of an open-vent volcano, Mount Etna, Italy. J. Geophys. Res. B:*  
11  
12 454 *Solid Earth 116 (10), B10204.*
- 14  
15 455 AIUPPA A. ET ALII (2015) - *New ground-based lidar enables volcanic CO<sub>2</sub> flux measurements. Sci.*  
16  
17 456 *Reports 5, 13614.*
- 19 457 AIUPPA A., LO COCO E., LIUZZO M., GIUDICE G., GIUFFRIDA G. & MORETTI R. (2016) - *Terminal*  
20  
21 458 *Strombolian activity at Etna's central craters during summer 2012: The most CO<sub>2</sub>-rich volcanic*  
22  
23 459 *gas ever recorded at Mount Etna. Geochemical Journal, 50 (2), 123-138.*
- 26 460 AIUPPA A., FISCHER T.P., PLANK T., ROBIDOUX P. & DI NAPOLI R. (2017) - *Along-arc, interarc and*  
27  
28 461 *arc-to-arc variations in volcanic gas CO<sub>2</sub>/S<sub>T</sub> ratios reveal dual source of carbon in arc*  
29  
30 462 *volcanism. Earth Science Reviews 168, 24–47.*
- 33 463 AIUPPA A., FISCHER T.P., PLANK T. & BANI P. (2019) - *CO<sub>2</sub> flux emissions from the Earth's most*  
34  
35 464 *actively degassing volcanoes, 2005–2015. Sci. Reports 9:5442, [https://doi.org/10.1038/s41598-](https://doi.org/10.1038/s41598-019-41901-y)*  
36  
37 465 *[019-41901-y](https://doi.org/10.1038/s41598-019-41901-y).*
- 40 466 ALLARD P., AIUPPA A., BEAUDICEL, GAUDIN D., DI NAPOLI R., CRISPI O., CALABRESE S., PARELLO  
41  
42 467 F., HAMMOUYA G., TAMBURELLO G. (2014) *Steam and gas emission rate from La Soufriere*  
43  
44 468 *volcano, Guadeloupe (Lesser Antilles): implications for the magmatic supply during degassing*  
45  
46 469 *unrest. Chemical Geology 384, 76–93*
- 49 470 ASIMOW P.D., DIXON J.E. & LANGMUIR C.H. (2004) - *A hydrous melting and fractionation model*  
50  
51 471 *for mid-ocean ridge basalts: application to the Mid-Atlantic Ridge near the Azores.*  
52  
53 472 *Geochemistry, Geophysics, Geosystems 5, doi:10.1029/2003GC000568.*
- 56 473 BONATTI E. (1990) - *Not so hot 'hot spots' in the oceanic mantle. Science 250, 107-111.*  
57  
58  
59  
60

1

2

3

4

5

6

7

8

9

10

11

12

13

14

15

16

17

18

19

20

21

22

23

24

25

26

27

28

29

30

31

32

33

34

35

36

37

38

39

40

41

42

43

44

45

46

47

48

49

50

51

52

53

54

55

56

57

58

59

60

- 474 BRUNE S., WILLIAMS S.E. & MÜLLER R.D. (2017) - *Potential links between continental rifting, CO<sub>2</sub>*  
475 *degassing and climate change through time*. Nat. Geosci., **10**, 941–946. doi: 10.1038/s41561-  
476 017-0003-6.
- 477 CALIRO S., VIVEIROS F., CHIODINI G. & FERREIRA T. (2015) - *Gas geochemistry of hydrothermal*  
478 *fluids of the S. Miguel and Terceira Islands, Azores*. Geochimica et Cosmochimica Acta, **168**,  
479 43-57. doi: 10.1016/j.gca.2015.07.009.
- 480 CAPPELLO A., GANCI G., CALVARI S., PÉREZ N.M., HERNÁNDEZ P.A., SILVA S.V., CABRAL J. & DEL  
481 NEGRO C. (2016) - *Lava flow hazard modeling during the 2014-2015 Fogo eruption, Cape*  
482 *Verde*. Journal of Geophysical Research: Solid Earth, **121** (4), pp. 2290-2303.
- 483 CARN S.A., FIOLETOV V.E., MCLINDEN C.A., LI C. & KROTKOV N.A. (2017) - *A decade of global*  
484 *volcanic SO<sub>2</sub> emissions measured from space*. Sci. Reports 7:44095, doi: 10.1038/srep44095.
- 485 CARRACEDO J.-C., PEREZ-TORRADO F.J., RODRIGUEZ-GONZALEZ A., PARIS R., TROLL V.R. &  
486 BARKER A.K. (2015) - *Volcanic and structural evolution of Pico do Fogo, Cape Verde*. Geology  
487 Today, **31** (4), pp. 146-152.
- 488 CHIODINI G. & MARINI L. (1998) - *Hydrothermal gas equilibria: The H<sub>2</sub>O-H<sub>2</sub>-CO<sub>2</sub>-CO-CH<sub>4</sub> system*.  
489 Geochim. Cosmochim. Acta, **62** (15), 2673-2687. doi: 10.1016/S0016-7037(98)00181-1.
- 490 CHRISTENSEN B., HOLM P., JAMBON A. & WILSON J. (2001) - *Helium, argon and lead isotopic*  
491 *composition of volcanics from Santo Antão and Fogo, Cape Verde Islands*. Chemical Geology,  
492 **178**, 127–142.
- 493 COURTNEY R.C. & WHITE R.S. (1986) - *Anomalous heat-flow and geoid across the Cape- Verde*  
494 *rise — evidence for dynamic support from a thermal plume in the mantle*. Geophysical Journal  
495 International, **87** (3), 815–867.
- 496 CROUGH S.T. (1978) - *Thermal origin of mid-plate hot-spot swells*. Geophys. J. R. Astron. Soc., **55**,  
497 451– 469.



- 1  
2  
3 498 CROUGH S.T. (1982) - *Geoid anomalies over the Cape Verde Rise*. Mar. Geophys. Res., **5**, 263–  
4  
5 499 271, doi:10.1007/BF00305564.  
6  
7  
8 500 DASGUPTA R. (2013). *Ingassing, storage, and outgassing of terrestrial carbon through geologic*  
9  
10 501 *time*. Rev. Mineral. Geochem., **75**, 183–229. doi: 10.2138/rmg.2013.75.7.  
11  
12 502 DASGUPTA R. & HIRSCHMANN M.M. (2010) - *The deep carbon cycle and melting in Earth's*  
13  
14 503 *interior*. Earth Planet. Sci. Lett., **298**, 1–13. doi: 10.1016/j.epsl.2010.06.039.  
15  
16  
17 504 DAVIES G.F., NORRY M.J., GERLACH D.C. & CLIFF R.A. (1989) - *A combined chemical and Pb-Sr-*  
18  
19 505 *Nd isotope study of the Azores and Cape Verde hotspots: The geodynamic implications, in*  
20  
21 506 *Magmatism in the Ocean Basins*. In Saunders A.D. & Norry M.J. Geol. Soc. Spec. Publ.,  
22  
23 **42**,231–255.  
24 507  
25  
26 508 Day, S.J., Heleno Da Silva, S.I.N., Fonseca, J.F.B.D. A past giant lateral collapse and present-day  
27  
28 509 flank instability of Fogo, Cape Verde Islands (1999) Journal of Volcanology and Geothermal  
29  
30 Research, 94 (1-4), pp. 191-218.  
31 510  
32  
33 511 Day, S.J., Carracedo, J., Guillou, H., Pais Pais, F., Rodriguez Badiola, E., Fonseca, J., Heleno da  
34  
35 512 Silva, S., 2000. Comparison and cross-checking of historical, archaeological and geological  
36  
37 513 evidence for the location and type of historical and sub-historical eruptions of multiple-vent  
38  
39 514 oceanic island volcanoes. In: McGuire, W., Griffiths, D., Hancock, P., Stewart, I. (Eds.), The  
40  
41 515 Archaeology of Geological Catastrophes: Geological Society, London, Special Publications,  
42  
43 516 London, pp. 281–306.  
44  
45  
46 517 DELLE DONNE D., AIUPPA A., BITETTO M., D'ALEO R., COLTELLI M., COPPOLA D., PECORA E.,  
47  
48 518 RIPEPE M. & TAMBURELLO G. (2019) - *Changes in SO<sub>2</sub> Flux regime at Mt. Etna captured by*  
49  
50 519 *automatically processed ultraviolet camera data*. Remote Sensing, **11** (10), art. no. 1201.  
51  
52  
53 520 DIONIS S.M., MELIÁN G., RODRÍGUEZ F., HERNÁNDEZ P.A., PADRÓN E., PÉREZ N.M., BARRANCOS J.,  
54  
55 521 PADILLA G., SUMINO H., FERNANDES P., BANDOMO Z., SILVA S., PEREIRA J.M. & SEMEDO H.  
56  
57  
58  
59  
60



1  
2  
3  
4  
5  
6  
7  
8  
9  
10  
11  
12  
13  
14  
15  
16  
17  
18  
19  
20  
21  
22  
23  
24  
25  
26  
27  
28  
29  
30  
31  
32  
33  
34  
35  
36  
37  
38  
39  
40  
41  
42  
43  
44  
45  
46  
47  
48  
49  
50  
51  
52  
53  
54  
55  
56  
57  
58  
59  
60

- 522 (2014) - *Diffuse volcanic gas emission and thermal energy release from the summit crater of*  
523 *Pico do Fogo, Cape Verde*. *Bulletin of Volcanology*, **77** (2), 13 p.
- 524 DIONIS S.M., PÉREZ N.M., HERNÁNDEZ P.A., MELIÁN G., RODRÍGUEZ F., PADRÓN E., SUMINO H.,  
525 BARRRANCOS J., PADILLA G.D., FERNANDES P., BANDOMO Z., SILVA S., PEREIRA J.M., SEMEDO,  
526 H. & CABRAL J. (2015) - *Diffuse CO<sub>2</sub> degassing and volcanic activity at Cape Verde Islands,*  
527 *West Africa*. *Earth, Planets and Space*, **67** (1), art. no. 48.
- 528 Doucelance R., Escrig S., Moreira M., Gariépy C. & Kurz M.D. (2003) - *Pb-Sr-He isotope and*  
529 *trace element geochemistry of the Cape Verde Archipelago*. *Geochim. Cosmochim. Acta*, **67**,  
530 3717–3733.
- 531 FERREIRA T. & OSKARSSON N. (1999) - *Chemistry and isotopic composition of fumarole discharges*  
532 *of Furnas caldera*. *J. Volcanol. Geotherm. Res.* **92**, 169–179.
- 533 FERREIRA T., GASPAR J.L., VIVEIROS F., MARCOS M., FARIA C. & SOUSA F. (2005) - *Monitoring of*  
534 *fumarole discharge and CO<sub>2</sub> soil degassing in the Azores: contribution to volcanic surveillance*  
535 *and public health risk assessment*. *Ann. Geophys.* **48**, 787–796.
- 536 FISCHER T.P. (2013) - *DEep CARbon DEgassing: The Deep Carbon Observatory DECADE*  
537 *Initiative*. *Mineralogical Magazine*, **77**(5), 1089.
- 538 FISCHER T.P. & AIUPPA A. (2020). *Global CO<sub>2</sub> emissions from subaerial volcanism: recent*  
539 *progresses and future challenges*. *Geochem. Geophys., Geosyst.*, under consideration.
- 540 FISCHER T.P. & CHIODINI G. (2015). *Volcanic, Magmatic and Hydrothermal Gases*. In: *The*  
541 *Encyclopedia of Volcanoes*, 2nd Edition, Edited by H. Sigurdsson, B. Houghton, S. McNutt, H.  
542 Rymer, J. Stix Elsevier, doi: 10.1016/B978-0-12-385938-9.00045-6
- 543 FISCHER T.P., ET ALII (2019) - *The emissions of CO<sub>2</sub> and other volatiles from the world's subaerial*  
544 *volcanoes*. *Sci. Rep.*, **9**:18716, <https://doi.org/10.1038/s41598-019-54682-1>.

- 1  
2  
3 545 GERLACH D.C., CLIFF C.A., DAVIES G.R., NORRY M.J. & HODGSON N. (1988) - *Magma sources of*  
4  
5 546 *the Cape Verdes archipelago: Isotopic and trace element constraints*. *Geochim. Cosmochim.*  
6  
7 547 *Acta*, **52**, 2979–2992. doi:10.1016/0016-7037(88)90162-7.  
9  
10 548 GERLACH T.M. (1991) - *Present-day carbon dioxide emissions from volcanoes*. *Earth in Space* 4, 5.  
11  
12 549 Global Volcanism Program, 2017. Report on Fogo (Cape Verde). In: Crafford A.E. & Venzke E.  
13  
14 (eds.), *Bulletin of the Global Volcanism Network*, **42**, 9. Smithsonian Institution.  
15 550 <https://doi.org/10.5479/si.GVP.BGVN201709-384010>.  
16  
17 551  
18  
19 552 GIGGENBACH W.F. (1987), *Redox processes governing the chemistry of fumarolic gas discharges*  
20  
21 553 *from White Island, New Zealand*, *Appl. Geochem.*, **2**, 143–161, doi:10.1016/0883-  
22  
23 2927(87)90030-8.  
24 554  
25  
26 555 HERNÁNDEZ P.A. (2015) - *Chemical composition of volcanic gases emitted during the 2014-15*  
27  
28 556 *Fogo eruption, Cape Verde*. *Geophysical Research Abstracts*, Vol. **17**, EGU2015-9577, 2015,  
29  
30 EGU General Assembly 2015.  
31 557  
32  
33 558 HILDNER E., KLÜGEL A. & HAUFF F. (2011) - *Magma storage and ascent during the 1995 eruption*  
34  
35 559 *of Fogo, Cape Verde Archipelago*. *Contributions to Mineralogy and Petrology*, **162 (4)**, 751.  
36  
37 560 doi:10.1007/s00410-011-0623-6.  
38  
39  
40 561 HILDNER H., KLÜGEL A. & HANSTEEN T. (2012) - *Barometry of lavas from 1951 eruption of Fogo,*  
41  
42 562 *Cape Verde Islands: implications for historic and prehistoric magma plumbing system*. *Journal*  
43  
44 563 *of Volcanology and Geothermal Research*, **217-218**, 73–90.  
45  
46  
47 564 HOERNLE K., TILTON G., LE BAS M.J., DUGGEN S. & GARBE-SCHÖNBERG D. (2002) - *Geochemistry*  
48  
49 565 *of oceanic carbonatites compared with continental carbonatites: mantle recycling of oceanic*  
50  
51 566 *crustal carbonate*. *Contributions to Mineralogy and Petrology*, **142(5)**, 520-542.  
52  
53  
54 567 HOLM P.M., WILSON J.R., CHRISTENSEN B.P., HANSEN L., HANSEN S.L., HEIN K.M., MORTENSEN  
55  
56 568 A.K., PEDERSEN R., PLESNER S. & RUNGE M.K. (2006) - *Sampling the Cape Verde mantle plume:*  
57  
58  
59  
60

1  
2  
3  
4  
5  
6  
7  
8  
9  
10  
11  
12  
13  
14  
15  
16  
17  
18  
19  
20  
21  
22  
23  
24  
25  
26  
27  
28  
29  
30  
31  
32  
33  
34  
35  
36  
37  
38  
39  
40  
41  
42  
43  
44  
45  
46  
47  
48  
49  
50  
51  
52  
53  
54  
55  
56  
57  
58  
59  
60

- 569 *evolution of the melt compositions on Santo Antão, Cape Verde Islands*. *Journal of Petrology*, **47**,
- 570 145–189.
- 571 HOLM P.M., GRANDVUINET T., FRIIS J., WILSON J.R., BARKER A.K. & PLESNER S. (2008) - *An  $^{40}\text{Ar}$ -*
- 572  *$^{39}\text{Ar}$  study of the Cape Verde hot spot: temporal evolution in a semistationary plate environment*.
- 573 *Journal of Geophysical Research* **113 (B8)**, B08201.
- 574 KANTZAS E.P., MCGONIGLE A.J.S., TAMBURELLO G., AIUPPA A. & BRYANT R.G. (2010) - *Protocols*
- 575 *for UV camera volcanic  $\text{SO}_2$  measurements*. *J. Volcanol. Geotherm. Res.*, **194**, 55–60.
- 576 KERN C., KICK F., LÜBCKE P., VOGEL L., WÖHRBACH M. & AND PLATT U. (2010) - *Theoretical*
- 577 *description of functionality, applications, and limitations of  $\text{SO}_2$  cameras for the remote sensing*
- 578 *of volcanic plumes*. *Atmos. Meas. Tech.*, **3**, 733–749, [www.atmos-meas-tech.net/3/733/2010/](http://www.atmos-meas-tech.net/3/733/2010/)
- 579 [doi:10.5194/amt-3-733-2010](https://doi.org/10.5194/amt-3-733-2010).
- 580 KOGARKO L.N., RYABUKHIN V.A. & VOLYNETS M.P. (1992), *Cape Verde Island carbonatite*
- 581 *geochemistry*. *Geochem. Int.*, **29**, 62–74.
- 582 ILYINSKAYA E, AIUPPA A, BERGSSON B ET ALII (2015) - *Degassing regime of Hekla volcano 2012-*
- 583 *2013*. *Geochim. Cosmochim. Acta*, **159**. 80-99.
- 584 ILYINSKAYA E., MOBBS S., BURTON R., BURTON M., PARDINI F., PFEFFER M.A., ET ALII (2018) -
- 585 *Globally significant  $\text{CO}_2$  emissions from Katla, a Subglacial Volcano in Iceland*. *Geophys. Res.*
- 586 *Lett.*, **45**, 332–310. doi: 10.1029/2018GL079096.
- 587 LIU X. & ZHAO D. (2014) - *Seismic evidence for a mantle plume beneath the Cape Verde hotspot*.
- 588 *International Geology Review*, **56**, 1213–1225.
- 589 LOPEZ T., ET ALII, (2017) - *Geochemical constraints on volatile sources and subsurface conditions*
- 590 *at Mount Martin, Mount Mageik, and Trident Volcanoes, Katmai*. *J. Volcanol. Geotherm. Res.*,
- 591 **347** 64–81, <https://doi.org/10.1016/j.jvolgeores.2017.09.001>.

- 1  
2  
3 592 MARQUES F.O., CATALÃO J.C., DEMETS C., COSTA A.C.G. & HILDENBRAND A. (2013) - *GPS and*  
4  
5 593 *tectonic evidence for a diffuse plate boundary at the Azores Triple Junction*. Earth and Planetary  
6  
7  
8 594 *Science Letters* **381**, 177-187.
- 9  
10 595 MARQUES F.O., HILDENBRAND A., VICTÓRIA S.S., CUNHA D. & DIAS, P. (2020) - *Caldera or flank*  
11  
12 596 *collapse in the Fogo volcano? What age? Consequences for risk assessment in volcanic islands*.  
13  
14  
15 597 *Journal of Volcanology and Geothermal Research* (in press),  
16  
17 598 <https://doi.org/10.1016/j.jvolgeores.2019.106686>
- 18  
19 599 MATA J., MOREIRA M., DOUCELANCE R., ADER M. & SILVA, L.C. (2010) - *Noble gas and carbon*  
20  
21 600 *isotopic signatures of Cape Verde oceanic carbonatites: implications for carbon provenance*.  
22  
23 601 *Earth and planetary Science Letters*, **291**, 70–83.
- 24  
25  
26 602 MATA J., MARTINS S., MATTIELLI N., MADEIRA J., FARIA B., RAMALHO R.S., SILVA P., MOREIRA M.,  
27  
28 603 CALDEIRA R., RODRIGUES J. & MARTINS L. (2017) - *The 2014–15 eruption and the short-term*  
29  
30 604 *geochemical evolution of the Fogo volcano (Cape Verde): Evidence for small-scale mantle*  
31  
32  
33 605 *heterogeneity*. *Lithos*, **288–289**, 91–107.
- 34  
35 606 MELIÁN G., TASSI F., PÉREZ N., HERNÁNDEZ P., SORTINO F., VASELLI O., PADRÓN E., NOLASCO D.,  
36  
37 607 BARRANCOS J., PADILLA G., RODRÍGUEZ F., DIONIS S., CALVO D., NOTSU K. & SUMINO H. (2012)  
38  
39 608 - *A magmatic source for fumaroles and diffuse degassing from the summit crater of Teide*  
40  
41  
42 609 *Volcano (Tenerife, Canary Islands): A geochemical evidence for the 2004-2005 seismic-volcanic*  
43  
44 610 *crisis*. *Bulletin of Volcanology*, **74 (6)**, 1465-1483.
- 45  
46 611 MELIÁN G.V., ET ALII (2015) - *Insights from fumarole gas geochemistry on the recent volcanic*  
47  
48 612 *unrest of Pico do Fogo, Cape Verde*. *Geophysical Research Abstracts*, Vol. **17**, EGU2015-  
49  
50 613 12754, 2015, EGU General Assembly 2015.
- 51  
52  
53 614 MÉTRICH N., ZANON V., CRÉON L., HILDENBRAND A., MOREIRA M., MARQUES F.O. (2014) - *Is the*  
54  
55 615 *“Azores hotspot” a wet spot? Insights from geochemistry of fluid and melt inclusions in olivines*  
56  
57 616 *of Pico basalts*. *J. Petrol.* **55**, 377-393
- 58  
59  
60

- 1  
2  
3 617 MILLET M.A., DOUCELANCE R., SCHIANO P., DAVID K. & BOSQ C. (2008) - *Mantle plume*  
4  
5 618 *heterogeneity versus shallow-level interactions: a case study, the São Nicolau Island, Cape*  
6  
7 *Verde archipelago*. Journal of Volcanology and Geothermal Research, **176(2)**, 265-276.  
8 619  
9  
10 620 MONTELLI R., NOLET G., DAHLEN F.A. & MASTERS G. (2006) - *A catalogue of deep mantle plumes:*  
11  
12 621 *new results from finite-frequency tomography*. Geochemistry, Geophysics, Geosystems **7**,  
13  
14 622 <http://dx.doi.org/10.1029/2006GC001248>  
15  
16  
17 623 MOURÃO, C., MOREIRA, M., MATA, J., RAQUIN, A., MADEIRA, J (2012) *Primary and secondary*  
18  
19 624 *processes constraining the noble gas isotopic signatures of carbonatites and silicate rocks from*  
20  
21 625 *Brava Island: evidence for a lower mantle origin of the Cape Verde plume*. Contributions to  
22  
23 *Mineralogy and Petrology* **163**, 995–1009.  
24 626  
25  
26 627 PEDONE M. ET ALII (2014) - *Volcanic CO<sub>2</sub> flux measurement at Campi Flegrei by tunable diode*  
27  
28 628 *laser absorption spectroscopy*. Bulletin of Volcanology, **76**, 13.  
29  
30  
31 629 QUEIBER M., GRANIERI D. & BURTON M. (2016) - *A new frontier in CO<sub>2</sub> flux measurements using a*  
32  
33 630 *highly portable DIAL laser system*. Scientific Reports, **6**, 33834.  
34  
35 631 RIBEIRO O. (1960) - *A Ilha do Fogo e as suas erupções (The island of Fogo and its eruptions)*. 2<sup>nd</sup>  
36  
37 632 *edn. Memórias, serie geographica I. Junta de Investigações do Ultramar. Ministerio do Ultramar,*  
38  
39 *Lisbon.*  
40 633  
41  
42 634 RICHTER N., FAVALLI M., DE ZEEUW-VAN DALFSEN E., FORNACIAI A., DA SILVA FERNANDES R.M.,  
43  
44 635 PÉREZ N.M., LEVY J., VICTÓRIA S.S. & WALTER T.R. (2016) - *Lava flow hazard at Fogo*  
45  
46 636 *Volcano, Cabo Verde, before and after the 2014-2015 eruption*. Natural Hazards and Earth  
47  
48 *System Sciences*, **16 (8)**, pp. 1925-1951.  
49 637  
50  
51 638 Saki, M., Thomas, C., Nippress, S.E.J., Lessing, S., 2015. *Topography of upper mantle seismic*  
52  
53 639 *discontinuities beneath the North Atlantic: the Azores, Canary and Cape Verde plumes*. Earth  
54  
55 and Planetary Science Letters **409**, 193–202  
56 640  
57  
58  
59  
60

- 1  
2  
3 641 TAMBURELLO G. (2015) - *Ratiocalc: Software for processing data from multicomponent volcanic*  
4  
5 642 *gas analyzers*. Comput. Geosci., **82**, 63–67.
- 7  
8 643 TAMBURELLO G., KANTZAS E.P., MCGONIGLE A.J.S. & AIUPPA A. (2011) - *Vulcamera, a program*  
9  
10 644 *for measuring volcanic SO<sub>2</sub> using UV cameras*. Ann. Geophys. **54**, 2.
- 12  
13 645 TAMBURELLO G., AIUPPA A., KANTZAS E.P., MCGONIGLE A.J.S. & RIPEPE M. (2012) - *Passive vs.*  
14  
15 646 *active degassing modes at an open-vent volcano (Stromboli, Italy)*. Earth Planet. Sci. Lett., **359–**  
16  
17 647 **360**, 106–116.
- 19  
20 648 TAMBURELLO G., MOUNE S., ALLARD P., VENUGOPAL S., ROBERT V., ROSAS-CARNAJAL M.,  
21  
22 649 UCCIANI G., DEROUSSI S, KITOU T., DIDIER T., KOMOROWSKI J-C., BEAUDICEL F., DE CHABALIER  
23  
24 650 J-B., LEMARCAHND A., MORETTI R., DESSERT C. (2019) *Spatio-temporal relationships between*  
25  
26 651 *fumarolic activity, hydrothermal fluid circulation and geophysical signals at an arc volcano in*  
27  
28 652 *degassing unrest: La Soufrière of Guadeloupe (French West Indies)*. Geosciences, **9**, 480-507  
29  
30 653 doi:10.3390/geosciences9110480.
- 32  
33 654 TARAN, Y., KALACHEVA, E. (2019) - *Role of hydrothermal flux in the volatile budget of a*  
34  
35 655 *subduction zone: Kuril arc, northwest Pacific*. Geology, 47 (1), 87-90. doi: 10.1130/G45559.1
- 37  
38 656 TARAN, Y.A. (2009) - *Geochemistry of volcanic and hydrothermal fluids and volatile budget of the*  
39  
40 657 *Kamchatka-Kuril subduction zone* Geochimica et Cosmochimica Acta, 73 (4), 1067-1094. , doi:  
41  
42 658 10.1016/j.gca.2008.11.020
- 44  
45 659 VAN DER MEER D.G., ZEEBE R.E., VAN HINSBERGEN D.J.J., SLUIJS A., SPAKMAN W. & TORSVIK T.H.  
46  
47 660 (2014) - *Plate tectonic controls on atmospheric CO<sub>2</sub> levels since the Triassic*. Proc. Natl. Acad.  
48  
49 661 *Sci. U.S.A.* 111, 4380–4385. doi:10.1073/pnas.1315657111.
- 51  
52 662 WERNER C., EVANS W. C., POLAND M., TUCKER D.S. & DOUKAS M.P. (2009) - *Long-term changes*  
53  
54 663 *in quiescent degassing at Mount Baker Volcano, Washington, USA; evidence for a stalled*  
55  
56 664 *intrusion in 1975 and connection to a deep magma source*. Journal of Volcanology and  
57  
58 665 *Geothermal Research* **186**, 379–386.
- 59  
60



1  
2  
3 666 WERNER C., ET ALII, (2019) - *Carbon Dioxide Emissions from Subaerial Volcanic Regions: Two*  
4  
5 667 *Decades in Review*. In: Orcutt B.N, Daniel I. & Dasgupta R. *Deep Carbon, Past to Present*.  
6  
7 Cambridge University Press [www.cambridge.org/9781108477499](http://www.cambridge.org/9781108477499), doi:  
8 668  
9 10.1017/9781108677950.  
10 669  
11

12 670 WONG K, MASON E., BRUNE S, EAST M., EDMONDS M. & ZAHIROVIC S. (2019) - *Deep Carbon*  
13  
14 *Cycling Over the Past 200 Million Years: A Review of Fluxes in Different Tectonic Settings*.  
15 671  
16 Front. Earth Sci. **7**, 263. doi: 10.3389/feart.2019.00263.  
17 672  
18

19 673  
20

## 21 674 **FIGURE CAPTIONS**

22  
23  
24 675 **Figure 1** - Google Earth image (Image © 2019 Maxar Technologies) of (a) the Cape Verde  
25  
26 676 archipelago and (b) Fogo Island.

27  
28 677 **Figure 2** – (a) Panoramic view of Pico do Fogo volcano; (b) Map of the Pico do Fogo summit  
29  
30 crater, showing (i) a thermal map of the fumarolic field; (ii) the position of the 17 analysed  
31 678 fumaroles (red circles, see (e) for a detail; white numbers identify fumaroles 1, 8 and 17 for  
32  
33 679 reference); (iii) the UV Camera measurement site (FOV and “cross section” are the Field of View  
34  
35 680 of the camera and the ICA integration section, respectively); and (iv) the Bulk-plume Multi-Gas  
36  
37 681 measurement site. The base map is from Bing Maps (<https://www.bing.com/maps>, Microsoft Ltd);  
38  
39 682 (c) the inner crater seen from the Bulk-plume Multi-Gas measurement site; (d) the fumarolic field  
40  
41 683 seen from the UV Camera measurement site. The plume transport direction is indicated by white  
42  
43 684 arrows. The position of some selected fumaroles (red circles with identification numbers) are shown  
44  
45 685 for reference; (e) A zoom of the inner crater (base map as in (a)), showing the track of the Multi-  
46  
47 686 GAS walking traverse and the positions of the 17 fumaroles (red circles with white labels; see Tab 1  
48  
49 687 for GPS positions). All measurements were performed on February 5, 2019.  
50  
51 688

52  
53  
54 689 **Figure 3** – Scatter plots of H<sub>2</sub>O, CO<sub>2</sub>, SO<sub>2</sub> and H<sub>2</sub> concentrations vs H<sub>2</sub>S in the plumes of  
55  
56 690 summit crater fumaroles at Pico do Fogo. Open circles stand for the 4446 concentration  
57  
58  
59  
60



1  
2  
3 691 measurements performed during the ~74-minute-long Multi-GAS walking traverse. H<sub>2</sub>O, CO<sub>2</sub> and  
4  
5 692 H<sub>2</sub> concentrations are corrected for air background (see text). In each plot, solid lines and grey-  
6  
7  
8 693 filled area identify the range (minimum, maximum) of X/H<sub>2</sub>S gas ratios in the identified 17  
9  
10 694 individual fumaroles (see Table 1). The large spread of compositions, indicated by the large ratio  
11  
12 695 interval (especially for the SO<sub>2</sub>/H<sub>2</sub>S ratio, varying from 0.001 to 1.5), attests to the chemical  
13  
14 696 heterogeneity of the fumarolic field. Otherwise, each of the 17 fumaroles exhibited stable, well-  
15  
16  
17 697 resolved X/H<sub>2</sub>S ratios, as here illustrated by the F15 fumarole example (grey-filled circles).

18  
19 698 **Figure 4** – Scatter plots of SO<sub>2</sub>/H<sub>2</sub>S ratios in the 17 fumaroles vs. (a) H<sub>2</sub>O/H<sub>2</sub>S ratios, (b)  
20  
21 699 H<sub>2</sub>O/CO<sub>2</sub> ratios, (c) CO<sub>2</sub>/S<sub>t</sub> ratios, and (d) H<sub>2</sub>/H<sub>2</sub>O ratios (data from Table 1). The SO<sub>2</sub>/H<sub>2</sub>S ratio is  
22  
23  
24 700 taken as a good indicator of the magmatic (high-SO<sub>2</sub>) vs. hydrothermal (high-H<sub>2</sub>S) signature of each  
25  
26 701 fumarole. The measured fumaroles define a nearly continuous trend between a “magmatic” gas end-  
27  
28 702 member, represented by the SO<sub>2</sub>-richer, hydrous (H<sub>2</sub>O/CO<sub>2</sub> ~ 2) and more oxidised (low H<sub>2</sub>/H<sub>2</sub>O)  
29  
30  
31 703 F14-F15 fumaroles, and a hydrothermal (H<sub>2</sub>S-dominated) end-member (exemplified by fumaroles  
32  
33 704 F3-F8), richer in CO<sub>2</sub> (CO<sub>2</sub>/S<sub>t</sub> > 130 and H<sub>2</sub>O/CO<sub>2</sub> < 1) and more reduced (H<sub>2</sub>/H<sub>2</sub>O > 0.0015). Note  
34  
35 705 that we directly collected 3 dry-gas samples of fumarole F15 for comparison, which yield a CO<sub>2</sub>/S<sub>t</sub>  
36  
37  
38 706 ratio range of 94-107 (Table 2; pink horizontal bar labelled “DS” in (c)) nearly identical to the  
39  
40 707 Multi-GAS-derived ratio (97; Table 1). In each plot the red star identifies the average (arithmetic  
41  
42 708 mean of the 17 fumaroles) composition of the fumarolic field (Table 1), while the vertical grey bar  
43  
44  
45 709 (“BULK”) indicates the SO<sub>2</sub>/H<sub>2</sub>S ratio measured in the bulk plume from the outer rim (site in Fig.  
46  
47 710 2).

48  
49 711 **Figure 5** – (a) SO<sub>2</sub> flux time-series obtained with the UV Camera from the “UV Camera”  
50  
51 712 measuring site indicated in Figure 2. Blue diamonds are individual data (obtained every 2 seconds)  
52  
53  
54 713 while the red line is for a 60 sec mobile average; (b) a pseudo-colour image obtained by  
55  
56 714 combination of two simultaneously taken (by the two co-exposed UV cameras) images, showing the  
57  
58 715 inner crater wall, and the ICA integration section (UV cross-section); (c) an example of SO<sub>2</sub> column  
59  
60

1  
2  
3  
4  
5  
6  
7  
8  
9  
10  
11  
12  
13  
14  
15  
16  
17  
18  
19  
20  
21  
22  
23  
24  
25  
26  
27  
28  
29  
30  
31  
32  
33  
34  
35  
36  
37  
38  
39  
40  
41  
42  
43  
44  
45  
46  
47  
48  
49  
50  
51  
52  
53  
54  
55  
56  
57  
58  
59  
60

716 amount (in ppm·m) variation along the camera pixels over the UV cross-section shown in (b). The  
717 plume is identified by higher-than-background SO<sub>2</sub> column amounts (0-400 ppm·m) between  
718 camera pixels 0 and ~200.

**Figure 6** – H<sub>2</sub>O/10-CO<sub>2</sub>-5S<sub>t</sub> triangular plot comparing the compositions of Pico do Fogo summit fumaroles (yellow circles, data from Table 1; red star mean composition as in Figure 4) with the compositions of (i) the 2014-2015 Fogo eruptive plume (orange circle labelled “FO”; HERNÁNDEZ *et alii*, 2015) (ii) hydrothermal vents from the Macaronesia (see legend) and worldwide (crosses; CHIODINI & MARINI, 1998). Also shown for comparison are the compositional fields of arc magmatic gases and intraplate/rift magmatic gases (AIUPPA, 2015). The white circles identify compositions for some intraplate /rift volcanoes (HE: Hekla; ER: Erebus; NY: Nyiragongo; KI: Kilauea summit; KE: Kilauea east rift zone; AR: Ardoukoba; PDF: Piton de la Fournaise; EA: Erta Ale; SU: Surtsey; see AIUPPA, 2015 for data provenance). Grey lines identify some characteristic CO<sub>2</sub>/S<sub>t</sub> and H<sub>2</sub>O/CO<sub>2</sub> ratios (see grey numbers on axes). The effects of S scrubbing, H<sub>2</sub>O condensation or addition are illustrated by the red lines (with arrows).

**Figure 7** – (a) Temperature dependence of CO<sub>2</sub>/S<sub>t</sub> (molar) ratios in the Macaronesia fumarolic gas samples. At Pico do Fogo, we measured temperatures (with a thermocouple) in only the three hottest vents (F5, F14 and F15). The CO<sub>2</sub>/S<sub>t</sub> (molar) ratios in hydrothermal fluids from volcanoes in the Azores and from Teide (Tenerife, Canary) are shown for comparison in both (a) and in the zoom of (b). The latter shows that CO<sub>2</sub>/S<sub>t</sub> ratios in fumaroles from Azores-Canary are negatively correlated with temperature, as observed globally (AIUPPA *et alii*, 2017). For reference, we also show in both panels the CO<sub>2</sub>/S<sub>t</sub> ratio signature of Fogo magmatic gas, as determined by Multi-GAS plume measurements during the 2014-2015 eruption (HERNÁNDEZ *et alii*, 2015; see also Figure 6).

**Figure 8** – Volatile outputs from different types of gas emissions on Fogo island: (i) the summit fumarolic field, this study; (ii) diffuse soil degassing from the crater area and the whole island

1  
2  
3 740 (DIONIS *et alii*, 2014, 2015); and (iii) eruptive degassing (HERNÁNDEZ *et alii*, 2015 and recalculated;  
4  
5 741 see text for explanation).

7  
8 742 **Figure 9** – Histogram showing the logarithmic distribution of the population of  
9  
10 743 measured/predicted CO<sub>2</sub> fluxes (in tons/day) from subaerial volcanoes. Data are from Fischer *et alii*,  
11  
12 744 (2019) except for Pico do Fogo (this study). Following FISCHER *et alii*, (2019) and FISCHER &  
13  
14 745 AIUPPA (2019, submitted), volcanoes are distinguished in two sub-categories: 1) Strong Volcanic  
16  
17 746 Gas Emitters (S<sub>vge</sub>, in red), including the 125 top degassing volcanoes whose SO<sub>2</sub> emissions have  
18  
19 747 systematically been detected from space-borne and/or ground-based spectrometers (CARN *et alii*,  
20  
21 748 2017; FISCHER *et alii*, 2019); and 2) Weak Volcanic Gas Emitters (W<sub>vge</sub>), including volcanoes with  
23  
24 749 no visible plumes and weak SO<sub>2</sub> emissions. Like in FISCHER *et alii*, (2019) and FISCHER & AIUPPA,  
25  
26 750 (2020, submitted), W<sub>vge</sub> are further divided into hydrothermal volcanoes, with minor to absent (< 8  
27  
28 751 tons/day) SO<sub>2</sub> emissions (yellow), and magmatic-hydrothermal volcanoes with somewhat higher (>  
30  
31 752 8 tons/day, but still undetectable from space) SO<sub>2</sub> emissions (orange). Pico do Fogo, although  
32  
33 753 falling in the subcategory of W<sub>vge</sub> (SO<sub>2</sub> < 8 tons/day) emits CO<sub>2</sub> at the upper W<sub>vge</sub> range, and at  
34  
35 754 levels comparable to (or higher than) many S<sub>vge</sub>.

**Table 1** – Results of Multi-GAS observations on Pico do Fogo fumarolic field on February 5, 2019. We report composition obtained for 17 fumaroles, the atmospheric plumes of which were measured for a few minutes each (time start – time end is GMT time). Temperature was measured in three fumaroles only using a portable thermocouple. For each fumarole, we report the peak SO<sub>2</sub> concentration (SO<sub>2</sub> max) measured during the acquisition interval and the volatile ratios (normalised to H<sub>2</sub>S) calculated with Ratiocalc (Tamburello, 2015) using the scatter-plot technique. For each ratio, mean is the slope of the best-fit regression line and R<sup>2</sup> is the corresponding correlation coefficient. We also report the recalculated molar percentages (mol. %) in the fumaroles and some representative molar ratios. \*Mean fumarole composition (and 1 standard deviation, 1 SD) calculated by averaging the compositions of the 17 fumaroles. The bulk plume was measured for its SO<sub>2</sub>/H<sub>2</sub>S ratio only from the crater rim site shown in Figure 2. †Ratios determined on the same F15 fumarole using direct sampling (data from Tab. 2).

Fumarole ID	T	LAT	LONG	Time Start	Time End	SO <sub>2</sub> max	Mean	R <sup>2</sup>	Error	Mean	R <sup>2</sup>	Error	Mean	R <sup>2</sup>	Error	Mean	R <sup>2</sup>	Error	mol%	mol%	mol%	mol%	mol%	molar	molar	molar	molar	
	°C					ppm	SO <sub>2</sub> /H <sub>2</sub> S	SO <sub>2</sub> /H <sub>2</sub> S	SO <sub>2</sub> /H <sub>2</sub> S	CO <sub>2</sub> /H <sub>2</sub> S	CO <sub>2</sub> /H <sub>2</sub> S	CO <sub>2</sub> /H <sub>2</sub> S	H <sub>2</sub> /H <sub>2</sub> S	H <sub>2</sub> /H <sub>2</sub> S	H <sub>2</sub> /H <sub>2</sub> S	H <sub>2</sub> O/H <sub>2</sub> S	H <sub>2</sub> O/H <sub>2</sub> S	H <sub>2</sub> O/H <sub>2</sub> S	H <sub>2</sub> O	CO <sub>2</sub>	H <sub>2</sub> S	SO <sub>2</sub>	H <sub>2</sub>	H <sub>2</sub> O/CO <sub>2</sub>	H <sub>2</sub> O/S <sub>tot</sub>	CO <sub>2</sub> /S <sub>t</sub>	H <sub>2</sub> /H <sub>2</sub> O	
1		14.95046	-24.34111	13:27	13:30	3.9	0.15	0.85	0.04	149	0.99	10	0.18	0.884	0.04	318	0.97	39	67.9	31.8	0.21	0.03	0.04	2.1	276	130	0.00057	
2		14.95063	-24.34071	13:31	13:32	4.9	0.16	0.65	0.12	136	0.96	30	0.13	0.848	0.06	260	0.97	49	65.5	34.2	0.25	0.04	0.03	1.9	224	117	0.00050	
3		14.95069	-24.34072	13:32	13:33	0.6	0.001	0.53	0.01	135	0.99	37	0.165	0.99	0.03	98	0.94	55	41.7	57.8	0.43	0.00	0.07	0.7	98	135	0.00169	
4		14.9507	-24.34072	13:33	13:36	3.8	0.05	0.53	0.03	117	0.94	20	0.13	0.677	0.06	184	0.90	59	61.0	38.6	0.33	0.02	0.04	1.6	175	111	0.00071	
5	225	14.95067	-24.3408	13:36	13:40	8.8	0.14	0.65	0.06	133	0.99	8	0.15	0.91	0.03	284	0.96	33	68.0	31.7	0.24	0.03	0.04	2.1	249	116	0.00053	
6		14.95066	-24.34072	13:41	13:46	5.2	0.36	0.90	0.22	134	0.99	7	0.18	0.918	0.03	277	0.96	27	67.2	32.4	0.24	0.09	0.04	2.1	203	98	0.00065	
7		14.95045	-24.34072	13:46	13:48	4.3	0.15	0.96	0.03	131	1.00	7	0.11	0.886	0.03	236	0.93	57	64.2	35.5	0.27	0.04	0.03	1.8	205	114	0.00047	
8		14.95032	-24.34078	13:49	13:51	5.1	0.03	0.78	0.01	167	0.99	12	0.24	0.949	0.04	116	0.61	80	40.8	58.7	0.35	0.01	0.08	0.7	113	163	0.00206	
9		14.95044	-24.34065	13:52	13:55	6.9	0.05	0.64	0.02	108	0.99	7	0.14	0.932	0.02	192	0.82	54	63.7	35.9	0.33	0.02	0.05	1.8	183	103	0.00073	
10		14.95061	-24.34068	13:57	14:00	35.2	0.79	0.85	0.21	207	0.98	18	0.15	0.82	0.04	404	0.92	74	65.9	33.7	0.16	0.13	0.02	2.0	226	115	0.00037	
11		14.95066	-24.34072	14:00	14:04	6.5	0.23	0.82	0.06	149	0.98	12	0.13	0.885	0.03	374	0.96	44	71.4	28.3	0.19	0.04	0.02	2.5	304	121	0.00035	
12		14.95067	-24.34085	14:04	14:11	1.4	0.2	0.86	0.03	176	0.98	9	0.16	0.395	0.08	356	0.87	56	66.7	33.1	0.19	0.04	0.03	2.0	296	147	0.00045	
13		14.95073	-24.34088	14:11	14:15	5.8	0.22	0.91	0.04	148	0.99	8	0.15	0.84	0.04	390	0.94	57	72.3	27.4	0.19	0.04	0.03	2.6	319	121	0.00038	
14	316	14.95064	-24.34064	14:17	14:18	24.7	0.85	0.33	1.42	172	0.70	134	0.05	0.144	0.14	311	0.62	283	64.1	35.5	0.21	0.18	0.01	1.8	168	93	0.00016	
15	315	14.95064	-24.34065	14:18	14:20	61.5	1.48	0.71	0.88	240	0.95	54	0.2	0.884	0.07 (0.09-0.1)†	482	0.97	73	66.5	33.2	0.14	0.20	0.03	2.0	194	97 (94-107)†	0.00042	
16		14.95062	-24.34061	14:21	14:25	14.2	0.45	0.83	0.11	160	0.98	13	0.14	0.916	0.02	442	0.89	81	73.2	26.6	0.17	0.07	0.02	2.8	305	111	0.00032	
17		14.95071	-24.34055	14:26	14:32	9.1	0.28	0.89	0.04	154	0.99	7	0.17	0.915	0.02	362	0.92	44	69.9	29.8	0.19	0.05	0.03	2.3	283	120	0.00047	
MEAN*							<b>0.3</b>			<b>153</b>			<b>0.2</b>			<b>299</b>			<b>64.1</b>	<b>35.6</b>	<b>0.2</b>	<b>0.06</b>	<b>0.04</b>	<b>1.9</b>	<b>225</b>	<b>118</b>	<b>0.00064</b>	
1 SD*							<b>0.4</b>			<b>33</b>			<b>0.04</b>			<b>109</b>			<b>9.2</b>	<b>9.1</b>	<b>0.08</b>	<b>0.06</b>	<b>0.02</b>	<b>0.6</b>	<b>67</b>	<b>18</b>	<b>0.00049</b>	
BULK		14.95073	-24.34196	11:37	12:01	0.15	0.12	0.70	0.04	-	-	-	-	-	-	-	-	-	-	-	-	-	-	-	-	-	-	-

**Table 2** - Chemistry (in mol %) of major and minor dry gas components in Pico do Fogo F15 fumarole. H<sub>2</sub>/H<sub>2</sub>S and CO<sub>2</sub>/H<sub>2</sub>S ratios are reported for comparison with the same ratios calculated by Multi-GAS

Sample	T °C	date	He ppm	H <sub>2</sub> ppm	O <sub>2</sub> %	N <sub>2</sub> %	CH <sub>4</sub> ppm	CO ppm	CO <sub>2</sub> %	H <sub>2</sub> S %	Tot %	H <sub>2</sub> /H <sub>2</sub> S	CO <sub>2</sub> /H <sub>2</sub> S
F15a	315	05/02/2019	8	952	0.11	0.51	0.7	15	97.03	1.03	98.8	0.09	94.20
F15b			8	979	0.33	1.4	1.3	17	95.83	0.96	98.6	0.10	99.82
F15c			6	373	12.63	46.35	2.1	13	39.6	0.37	99.0	0.10	107.03

**Table 3** - Volatile fluxes from Fogo island. All data in tons/day

	Summit Fumarolic Field*		Diffuse Degassing <sup>o</sup>		Eruptive degassing (2014 eruption) <sup>£</sup>	Eruptive degassing (time integrated) <sup>§</sup>
	Mean	1 SD	Mean	1 SD	Mean	Mean
<b>SO<sub>2</sub> flux</b>	1.4	0.4	-	-	10118	82
<b>H<sub>2</sub>O flux</b>	780	320	330	-	24245	196
<b>CO<sub>2</sub> flux</b>	1060	340	147-219 (828@)	35-36	10668	86
<b>H<sub>2</sub>S flux</b>	6.2	2.4	0.025	0.007	57	0.5
<b>H<sub>2</sub> flux</b>	0.05	0.022	0.033	0.0105	0.2	0.002

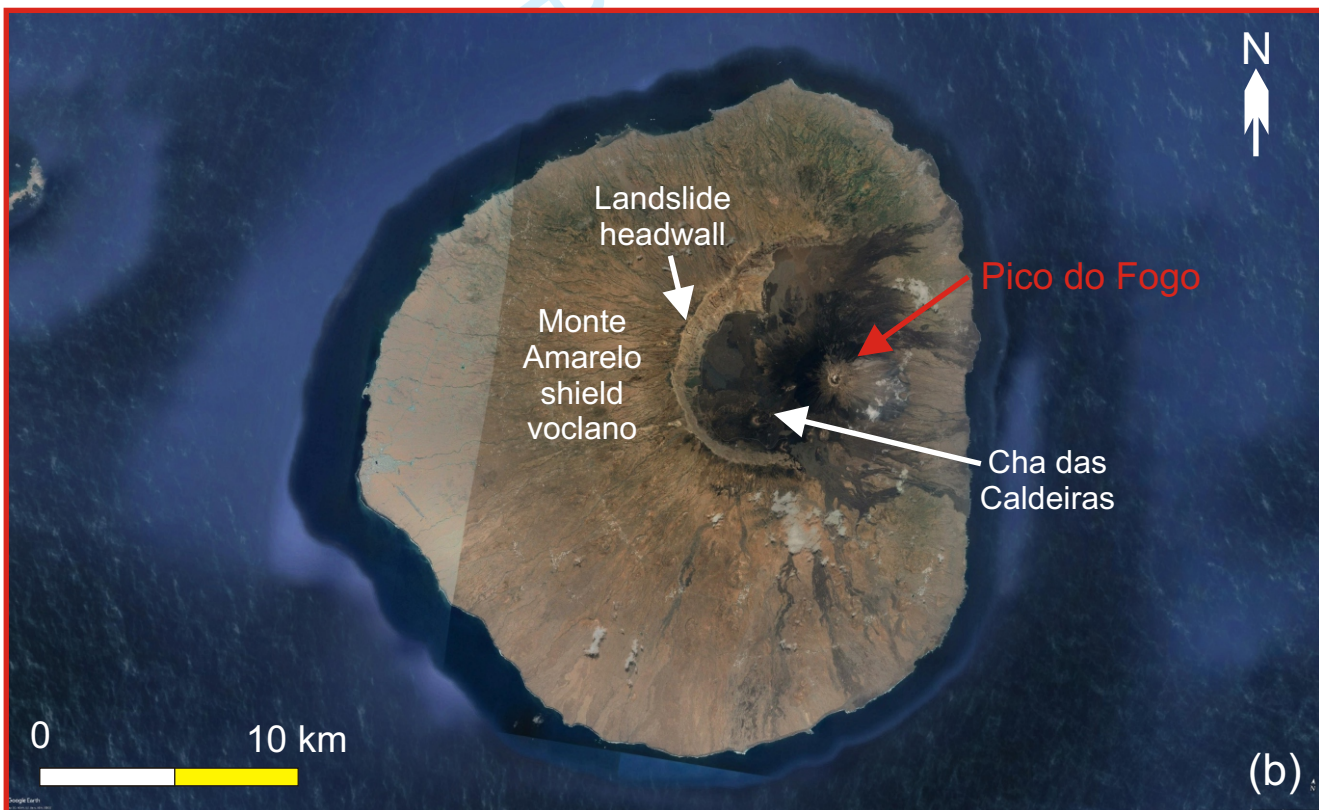
\*This work; <sup>o</sup>inner crater floor; Dionis et al., 2014; @whole island; Dionis et al., 2015; <sup>£</sup>Measured on November 30, 2014; Hernández et al., 2015; <sup>§</sup>This study, recalculated from data in Hernández et al., 2015



1  
2  
3  
4  
5  
6  
7  
8  
9  
10  
11  
12  
13  
14  
15  
16  
17  
18  
19  
20  
21  
22  
23  
24  
25  
26  
27  
28  
29  
30  
31  
32  
33  
34  
35  
36  
37  
38  
39  
40  
41  
42  
43  
44  
45  
46  
47  
48  
49  
50  
51  
52  
53  
54  
55  
56  
57  
58  
59  
60



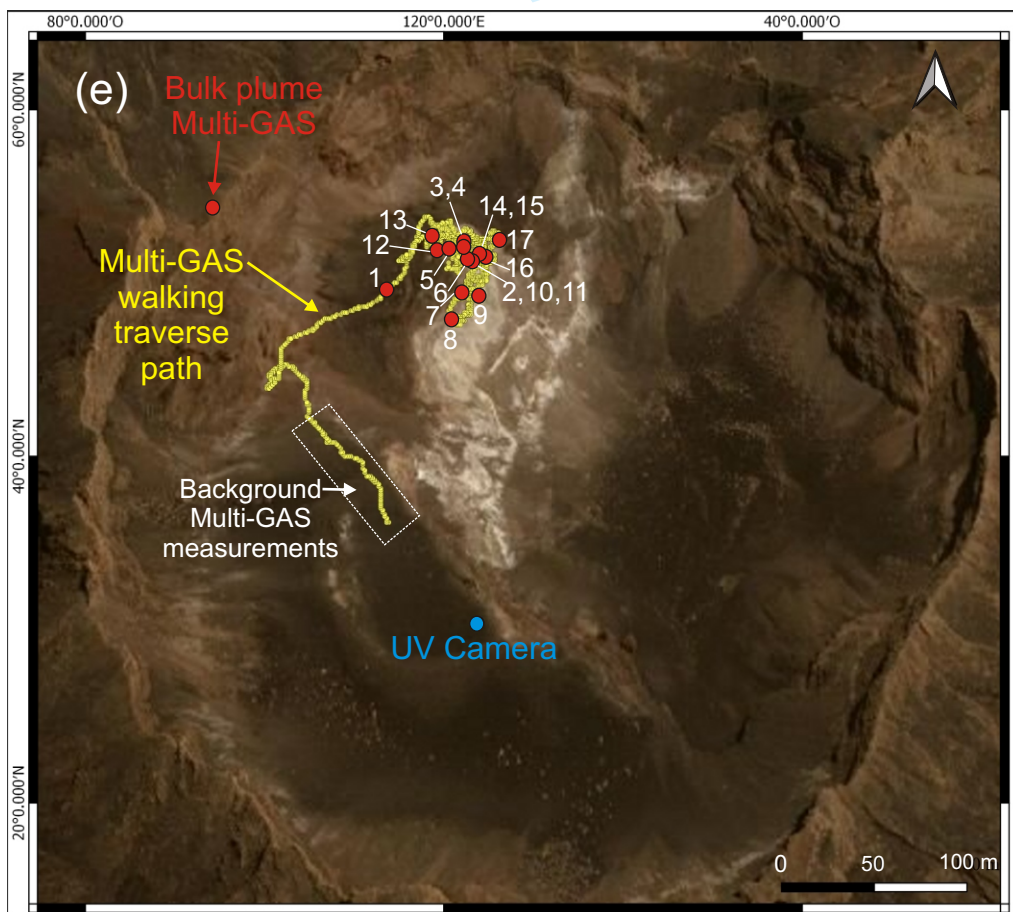
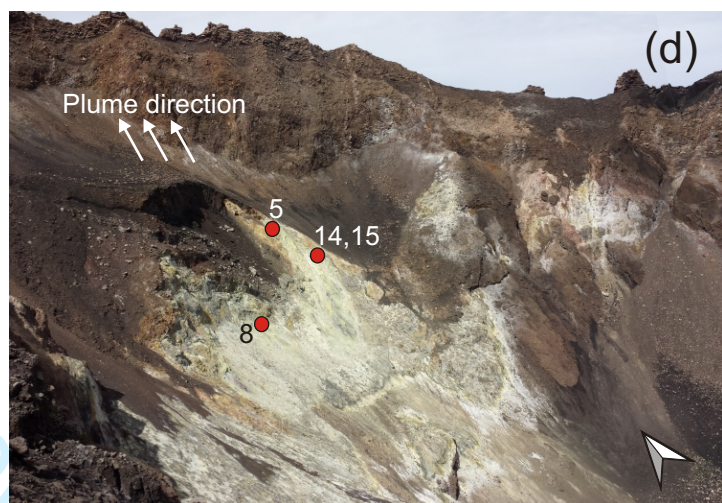
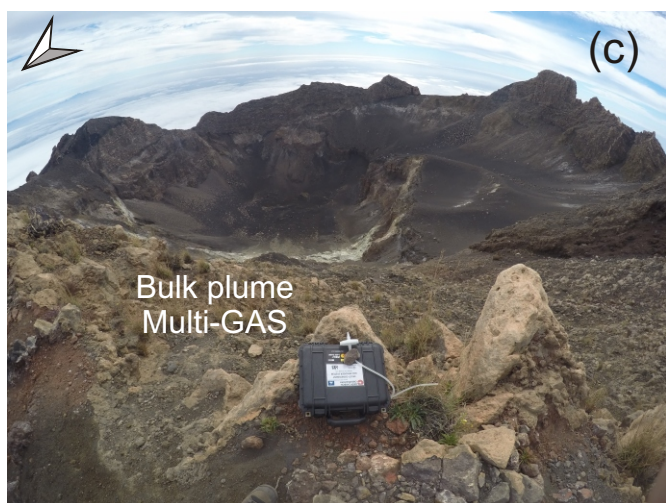
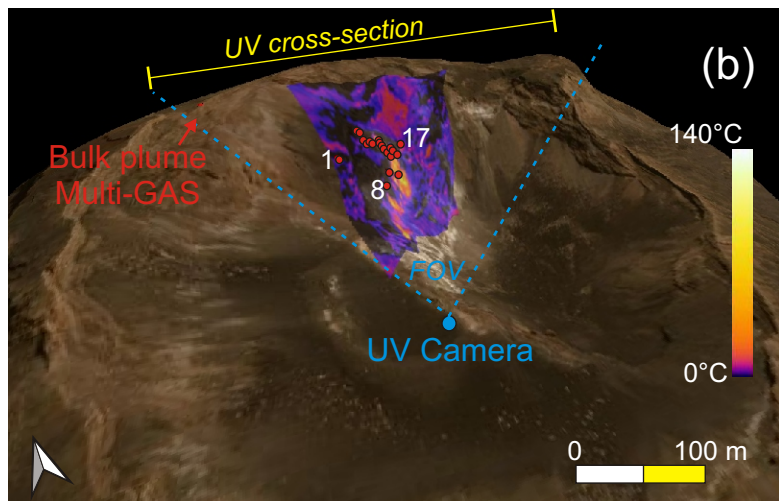
14°40'24"N



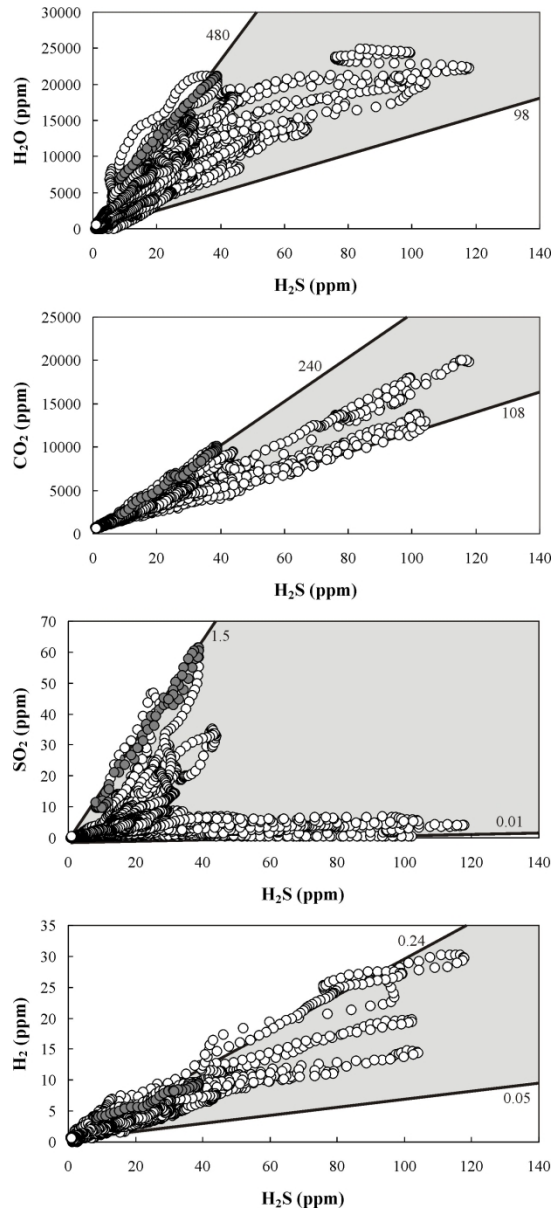
24°38'29"O

24°07'50"O



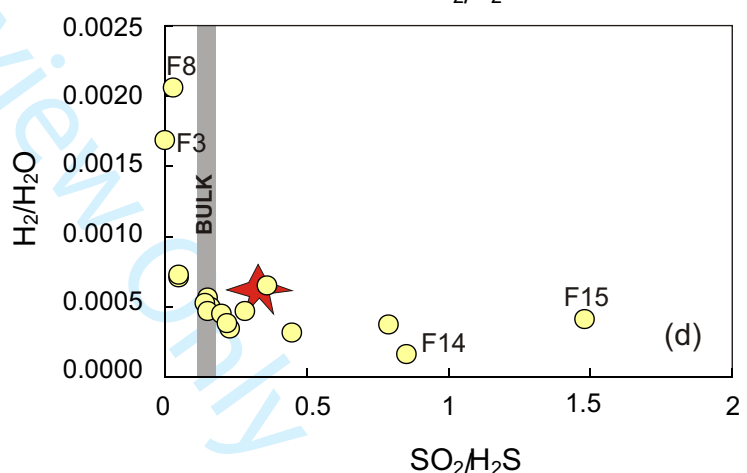
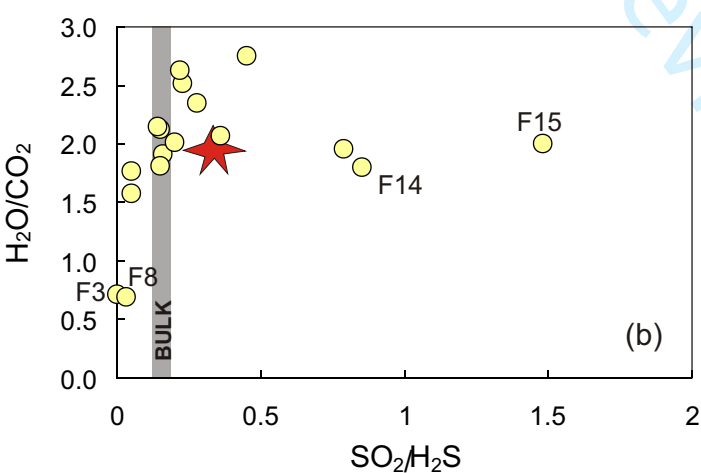
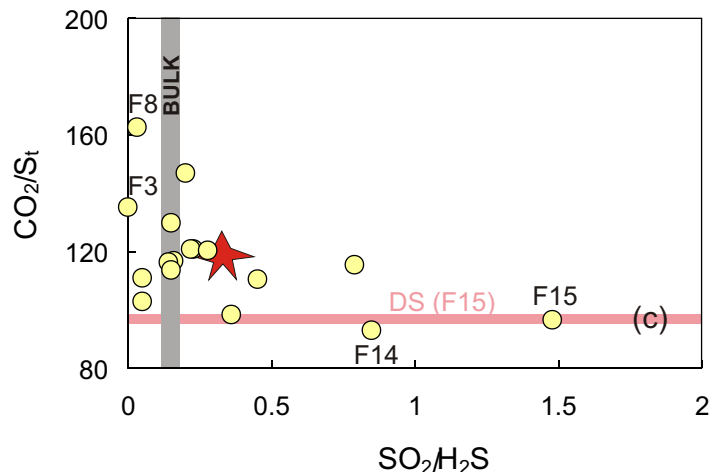
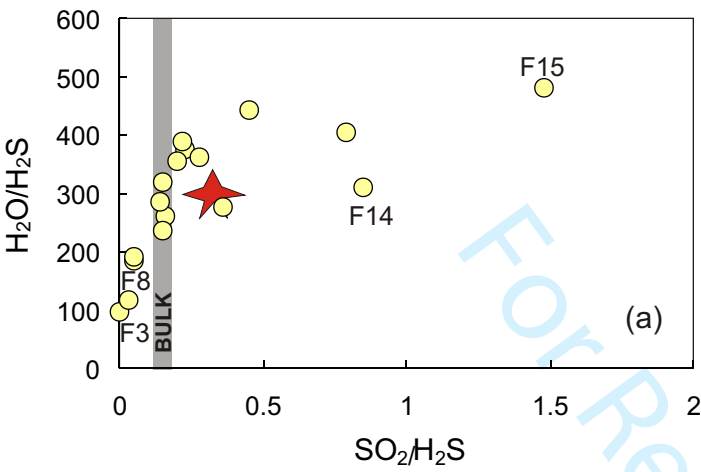


1  
2  
3  
4  
5  
6  
7  
8  
9  
10  
11  
12  
13  
14  
15  
16  
17  
18  
19  
20  
21  
22  
23  
24  
25  
26  
27  
28  
29  
30  
31  
32  
33  
34  
35  
36  
37  
38  
39  
40  
41  
42  
43  
44  
45  
46  
47  
48  
49  
50  
51  
52  
53  
54  
55  
56  
57  
58  
59  
60

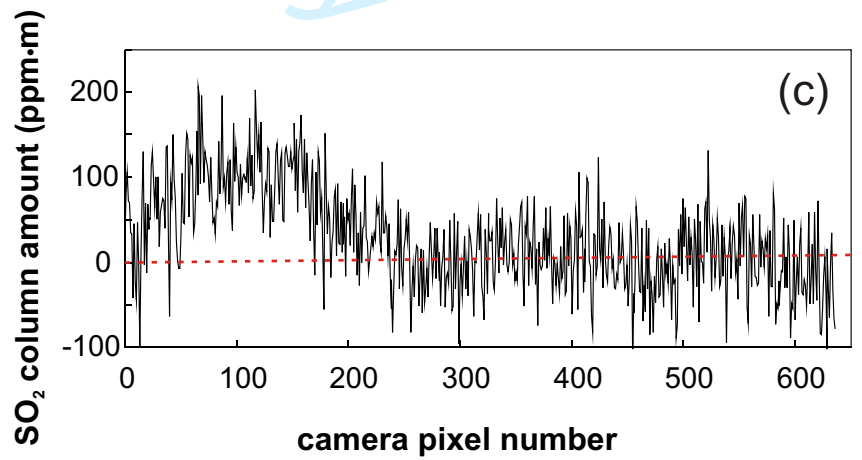
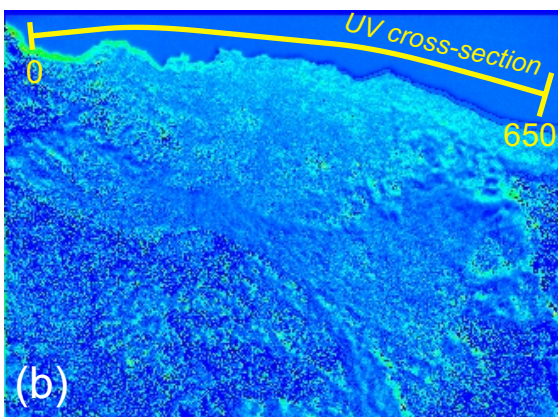
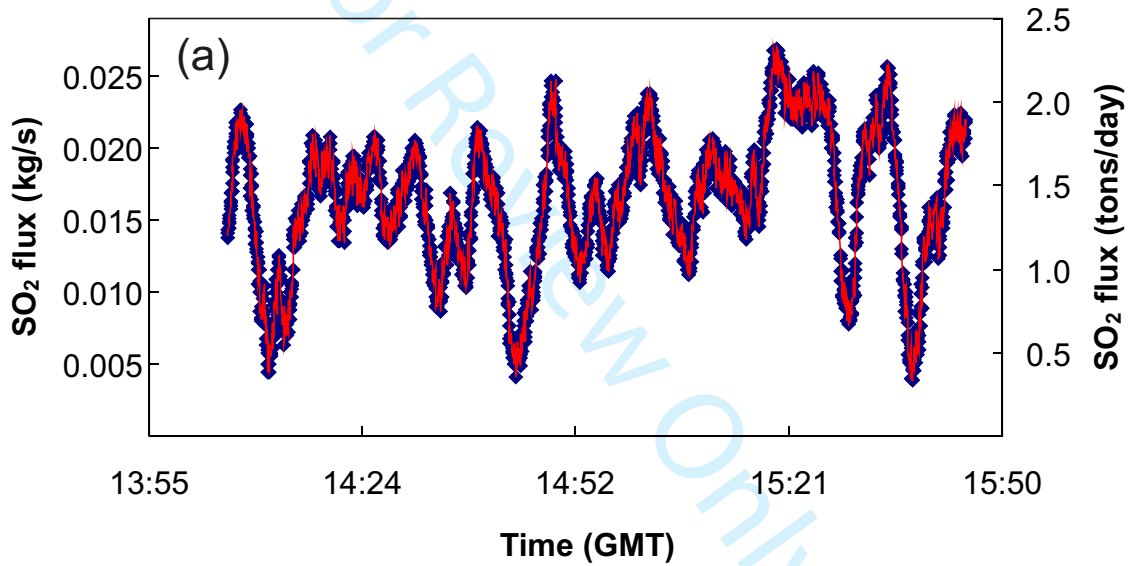


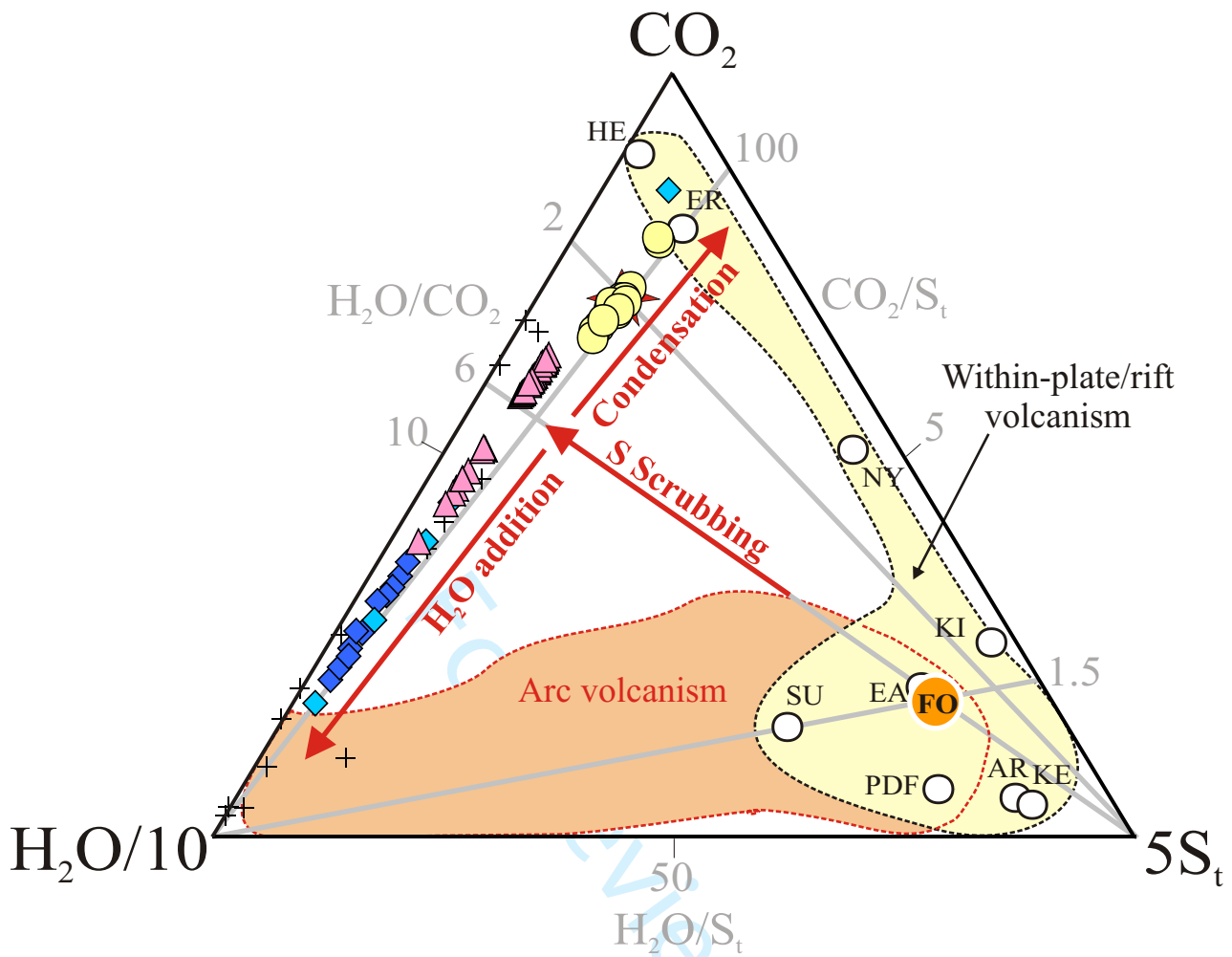
143x319mm (300 x 300 DPI)

1  
2  
3  
4  
5  
6  
7  
8  
9  
10  
11  
12  
13  
14  
15  
16  
17  
18  
19  
20  
21  
22  
23  
24  
25  
26  
27  
28  
29  
30  
31  
32  
33  
34  
35  
36  
37  
38  
39  
40  
41  
42  
43  
44  
45  
46  
47  
48  
49  
50  
51  
52  
53  
54  
55  
56  
57  
58  
59  
60









- Pico do Fogo summit fumaroles (this study)
- Fogo eruptive plume gas (Hernández et al., 2015)
- ★ Mean (Pico do Fogo) (this study)
- △ Canary (Teide) (Melian et al., 2012)
- ◆ Azores (Caliro et al., 2015)
- ◆ Azores (MARES Project, this study)
- Magmatic gases (intraplate/rift) (Aiuppa, 2015)
- + Hydrothermal gases (Chiodini and Marini, 1998)

